Electronic Supplementary Information for

Tetratopic Pyrimidine-Hydrazone Ligands Modified with Terminal Hydroxymethyl and Acryloyl Arms and their Pb(II), Zn(II), Cu(II) and Ag(I) Complexes

Daniel J. Hutchinson, Lyall R. Hanton, and Stephen C. Moratti*

Department of Chemistry, University of Otago, PO Box 56, Dunedin, New Zealand,

*E-mail: lhanton@chemistry.otago.ac.nz

Discussion of Disorder.

Figures S1-S7. Thermal ellipsoid views of precursor **AB**, ligand **L1** and complexes **1-5**.

Tables S1-S7. Selected bond lengths (Å) and angles (°) of precursor **AB**, ligand **L1** and complexes **1-5**.

Figures S8-S24. ^{1}H NMR spectra of precursor **AB**, ligands **L1** and **L2**, and their Pb(II), Zn(II) and Ag(I) complexes.

Figure S25-S32. ^{13}C NMR spectra of precursor **AB**, ligands **L1** and **L2**, and their Pb(II), Zn(II) and Ag(I) complexes.

Figure S33-S50. ESMS spectra of precursor **AB**, ligands **L1** and **L2**, and their Pb(II), Zn(II), Cu(II) and Ag(I) complexes.

Discussion of Disorder. The solid state structures of ligand **L1** and its Pb(II) complex $[Pb_2\mathbf{L1}(ClO_4)_2(CH_3CN)(H_2O)](ClO_4)_2 \cdot 2CH_3CN \cdot C_4H_{10}O \cdot H_2O$ (**3**) both contained significant electron density in the asymmetric unit which could not be resolved sufficiently. These electrons were therefore removed by the SQUEEZE procedure of PLATON. 52 electrons were removed from ligand **L1**, which corresponded to a CH_2Cl_2 molecule and a H_2O molecule. 42 electrons were removed from complex **3**, which corresponded to a CH_3CN molecule and two H_2O molecules.

Several of the crystal structures contained disordered components. One of the unbound ClO_4^- counterions in complex **3** was disordered over two sites with site occupancy factors of 0.55 and 0.45. Complex **5** contained a disordered phenyl ring (C21-C25) with site occupancy factors of 0.69 and 0.31. In addition, the O2 containing hydroxymethyl arm was also disordered over two sites with occupancy factors of 0.51 and 0.49. The hydrogens could not be located on the H_2O molecules of crystallization in $[Pb_4\mathbf{L1}(SO_3CF_3)_8]_2 \cdot 6CH_3CN \cdot H_2O$ (**2**) and complex **3**.

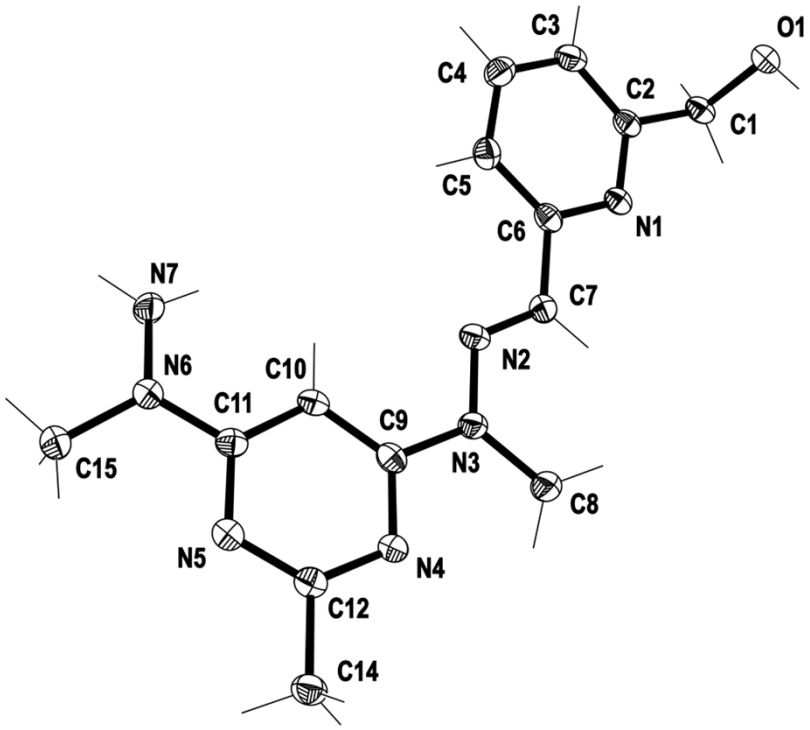

Figures S1. View of **AB** (crystallographic numbering). Thermal ellipsoids drawn at the 50 % probability level (the coordinated ClO_4^- anions have been removed for clarity).

Table S1. Selected bond lengths (Å) and angles (°) of **AB**.

C1-O1	1.432(3)	C11-N6	1.369(3)	N2-N3-C9	116.5(2)
C7-N2	1.293(3)	N6-N7	1.406(3)	N3-C9-N4	115.4(2)
N2-N3	1.356(3)	N1-C6-C7	114.1(2)	N5-C11-N6	115.7(2)
N3-C9	1.396(3)	C7-N2-N3	118.5(2)	C11-N6-N7	116.49(19)

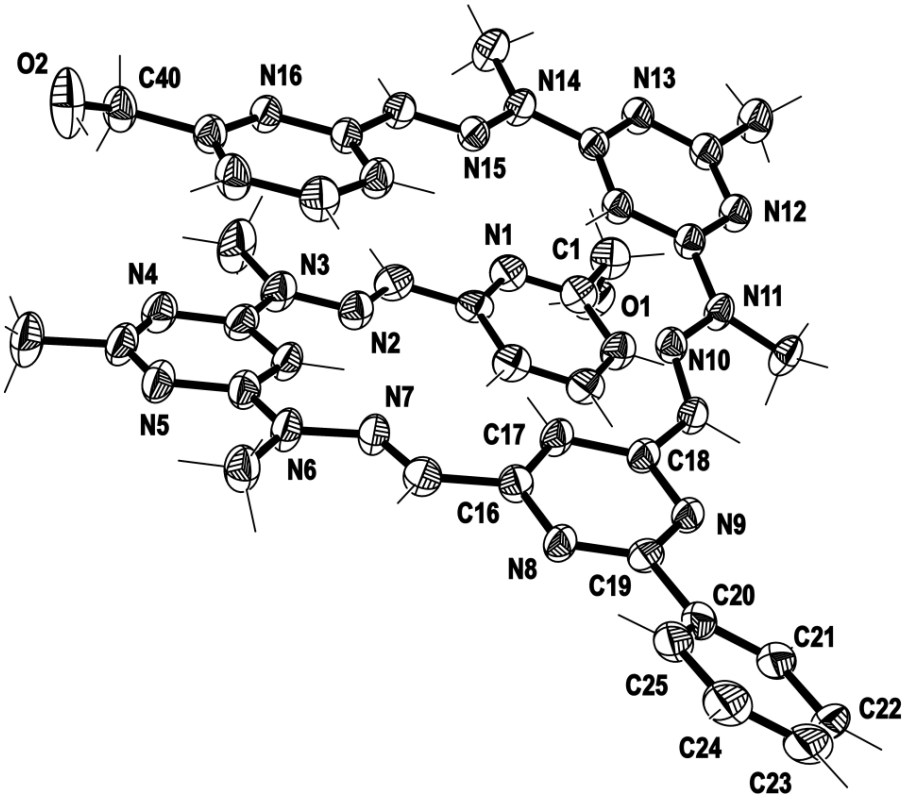

Figure S2. View of **L1** (crystallographic numbering). Thermal ellipsoids have been drawn at the 50 % probability level.

Table S2. Selected bond lengths (Å) and angles (°) of **L1**.

C1-O1	1.420(5)	C30-N14	1.399(4)	N7-C15-C16	119.4(3)
C7-N2	1.294(4)	N14-N15	1.359(4)	C15-C16-N8	113.9(3)
N2-N3	1.347(4)	N15-C34	1.281(4)	N9-C18-C26	114.2(3)
N3-C9	1.393(5)	C40-O2	1.398(4)	C18-C26-N10	120.9(3)
C11-N6	1.389(4)	N1-C6-C7	115.1(3)	N10-N11-C28	115.8(2)
N6-N7	1.361(4)	C7-N2-N3	120.0(3)	N11-C28-N12	114.9(3)
N7-C15	1.292(4)	N2-N3-C9	114.8(3)	N13-C30-N14	115.3(3)
C26-N10	1.283(4)	N3-C9-N4	116.8(3)	C30-N14-N15	115.4(2)
N10-N11	1.361(4)	N5-C11-N6	115.8(3)	N15-C34-C35	119.3(3)
N11-C28	1.401(4)	C11-N6-N7	114.2(3)	C34-C35-N16	115.0(3)

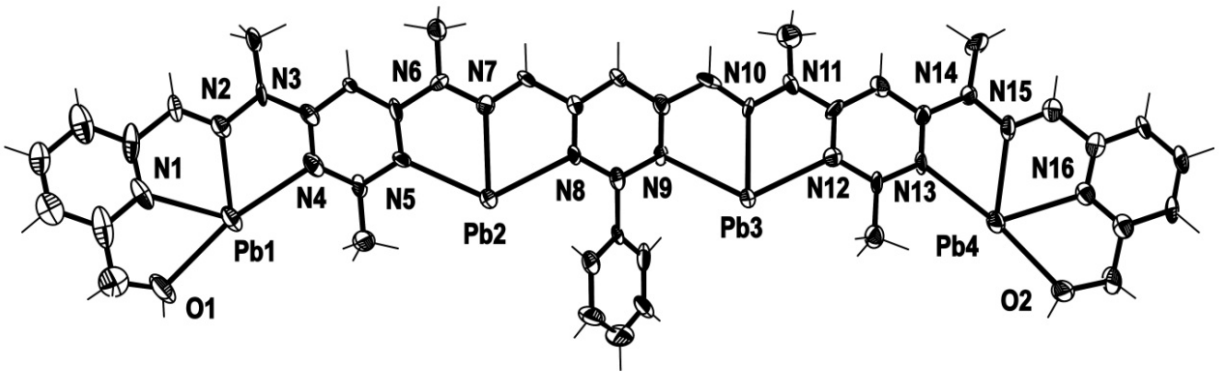

Figure S3. View of the $[Pb_4\mathbf{L1}(ClO_4)_7(H_2O)]^+$ cation of complex **1** (crystallographic numbering). Thermal ellipsoids drawn at the 50 % probability level (coordinated ClO_4^- anions and H_2O molecules have been removed for clarity).

Table S3. Selected bond lengths (Å) and angles (°) of $[Pb_4\mathbf{L1}(ClO_4)_7(H_2O)]ClO_4 \cdot 4CH_3NO_2$ (**1**)

Pb1-O1	2.601(12)	Pb3-N12	2.557(13)	O11-Pb1-O21	163.7(7)
Pb1-N1	2.498(17)	Pb3-O51	2.602(13)	N5-Pb2-N7	63.8(4)
Pb1-N2	2.570(14)	Pb3-O61	2.720(17)	N7-Pb2-N8	63.5(4)
Pb1-N4	2.720(13)	Pb3-O62	2.915(17)	N8-Pb2-O41	125.2(5)
Pb1-O11	2.727(12)	Pb4-N13	2.739(13)	N8-Pb2-N5	127.4(4)
Pb1-O14	2.893(12)	Pb4-N15	2.570(14)	O3-Pb2-O31	143.7(5)
Pb1-O21	2.57(3)	Pb4-N16	2.501(13)	N9-Pb3-N10	64.3(4)
Pb2-N5	2.532(13)	Pb4-O2	2.571(12)	N10-Pb3-N12	62.7(4)
Pb2-N7	2.548(13)	Pb4-O4	2.421(14)	N12-Pb3-N9	127.0(4)
Pb2-N8	2.591(12)	Pb4-O71	2.784(15)	O51-Pb2-O61	150.6(5)
Pb2-O3	2.525(13)	Pb4-O72	2.843(16)	N13-Pb4-N15	58.8(4)
Pb2-O31	2.550(13)	O1-Pb1-N1	62.3(6)	N15-Pb4-N16	65.5(5)
Pb2-O41	2.889(14)	N1-Pb1-N2	65.0(5)	N16-Pb4-O2	64.0(5)
Pb3-N9	2.596(12)	N2-Pb1-N4	59.9(5)	O2-Pb4-N13	155.4(4)
Pb3-N10	2.493(13)	N4-Pb1-O1	158.4(4)	O4-Pb4-O71	149.5(4)

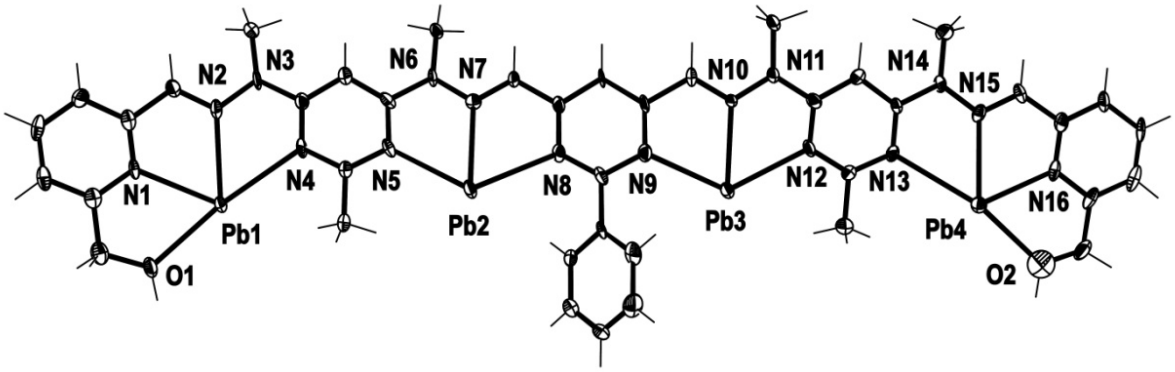

Figure S4. View of one of the $[Pb_4\mathbf{L1}(SO_3CF_3)_8]$ cations of complex **2** (crystallographic numbering. Thermal ellipsoids drawn at the 50 % probability level (the coordinated $SO_3CF_3^-$ anions have been removed for clarity).

Table S4. Selected bond lengths (Å) and angles (°) of $[Pb_4\mathbf{L1}(SO_3CF_3)_8]_2 \cdot 6CH_3CN \cdot H_2O$ (**2**)

Pb1-N1	2.523(11)	Pb3-O31	2.577(14)	N5-Pb2-N7	63.5(4)
Pb1-N2	2.614(13)	Pb3-O41	2.450(13)	N7-Pb2-N8	65.5(4)
Pb1-N4	2.735(11)	Pb3-O163	2.854(16)	N8-Pb2-N5	129.0(4)
Pb1-O1	2.552(10)	Pb4-N13	2.777(11)	N8-Pb2-O82	123.6(4)
Pb1-O11	2.451(11)	Pb4-N15	2.570(12)	O21-Pb2-O92	153.5(5)
Pb1-O121	2.708(11)	Pb4-N16	2.518(12)	N9-Pb3-N10	65.0(4)
Pb2-N5	2.540(12)	Pb4-O2	2.541(16)	N10-Pb3-N12	61.9(4)
Pb2-N7	2.506(12)	Pb4-O52	2.445(11)	N12-Pb3-N9	126.5(4)
Pb2-N8	2.629(11)	Pb4-O103	2.720(10)	N12-Pb3-O163	116.9(4)
Pb2-O21	2.497(12)	Pb4-O152	2.890(18)	O31-Pb3-O41	153.7(4)
Pb2-O82	2.875(18)	O1-Pb1-N1	64.6(4)	N13-Pb4-N15	59.9(4)
Pb2-O92	2.68(2)	N1-Pb1-N2	64.7(4)	N15-Pb4-N16	64.6(4)
Pb3-N9	2.654(12)	N2-Pb1-N4	57.7(4)	N16-Pb4-O2	63.4(5)
Pb3-N10	2.532(11)	N4-Pb1-O1	163.3(4)	O2-Pb4-N13	159.5(4)
Pb3-N12	2.557(11)	O11-Pb1-O121	161.7(4)	O52-Pb4-O103	157.1(3)

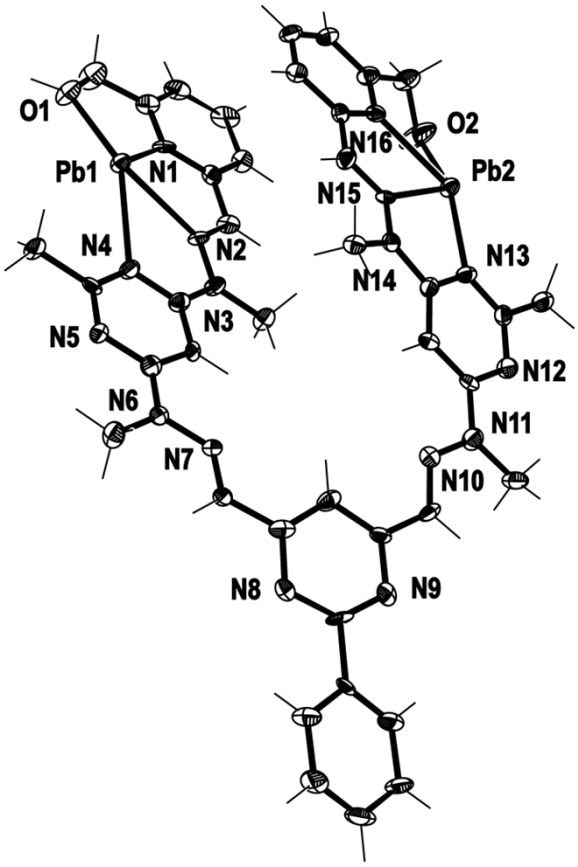

Figure S5. View of the $[Pb_2\mathbf{L1}(ClO_4)_2(CH_3CN)(H_2O)]^{2+}$ cation of complex **3**, (crystallographic numbering). Thermal ellipsoids drawn at the 50 % probability level (coordinated ClO_4^- anions, CH_3CN and H_2O molecules have been removed for clarity).

Table S5. Selected bond lengths (Å) and angles (°) of $[Pb_2\mathbf{L1}(ClO_4)_2(CH_3CN)(H_2O)](ClO_4)_2 \cdot 2CH_3CN \cdot C_4H_{10}O \cdot H_2O$ (**3**)

Pb1-N1	2.558(9)	Pb2-N16	2.496(8)	O21-Pb1-N17	148.7(4)
Pb1-N2	2.623(8)	Pb2-O2	2.724(10)	N13-Pb2-N15	61.0(3)
Pb1-N4	2.688(9)	Pb2-O3	2.486(8)	N15-Pb2-N16	65.1(3)
Pb1-O1	2.595(8)	Pb2-O11	2.696(8)	N16-Pb2-O2	63.1(3)
Pb1-O21	2.810(12)	O1-Pb1-N1	62.2(3)	O2-Pb2-N13	157.0(3)
Pb1-N17	2.645(11)	N1-Pb1-N2	63.8(3)	O3-Pb2-O11	143.9(3)
Pb2-N13	2.621(9)	N2-Pb1-N4	59.6(3)		
Pb2-N15	2.581(8)	N4-Pb1-O1	151.0(3)		

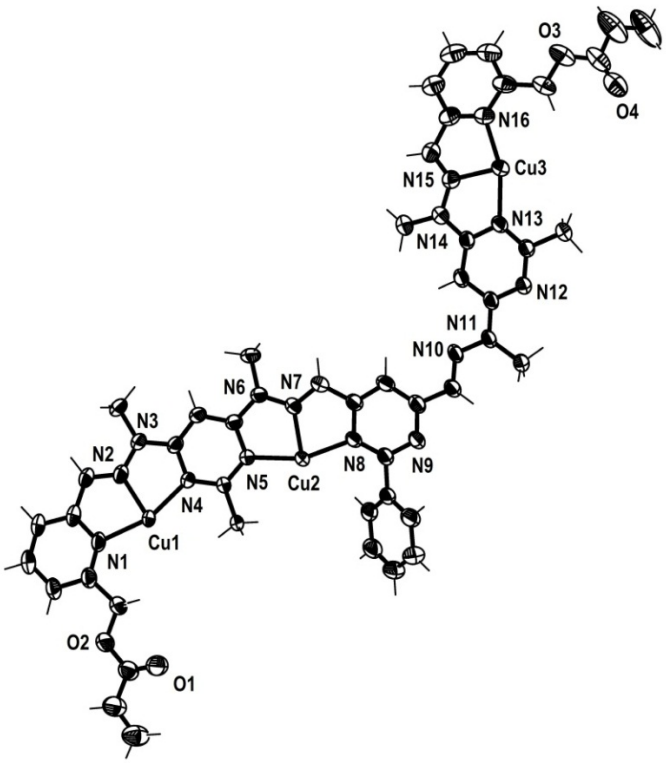

Figure S6. View of the $[Cu_3\mathbf{L2}(SO_3CF_3)_3(CH_3CN)_2(H_2O)]^{3+}$ cation of complex **4**, (crystallographic numbering). Thermal ellipsoids drawn at the 50 % probability level (coordinated ClO_4^- anions, CH_3CN and H_2O molecules have been removed for clarity).

Table S6. Selected bond lengths (Å) and angles (°) of $[Cu_3\mathbf{L2}(SO_3CF_3)_3(CH_3CN)_2(H_2O)](SO_3CF_3)_3\cdot 2CH_3CN\cdot H_2O$ (**4**).

Cu1-N1	2.040(4)	Cu3-N13	2.006(4)	N5-Cu2-N7	78.62(16)
Cu1-N2	1.947(4)	Cu3-N15	1.952(4)	N7-Cu2-N8	80.20(16)
Cu1-N4	2.014(4)	Cu3-N16	2.055(4)	N8-Cu2-N5	158.80(16)
Cu1-N17	1.980(4)	Cu3-O5	1.971(4)	N7-Cu2-N18	154.84(18)
Cu1-O11	2.196(4)	Cu3-O31	2.229(4)	N7-Cu2-O21	104.63(18)
Cu2-N5	2.064(4)	N1-Cu1-N2	80.84(17)	N13-Cu3-N15	79.72(17)
Cu2-N7	1.947(4)	N2-Cu1-N4	78.90(16)	N15-Cu3-N16	79.99(18)
Cu2-N8	2.061(4)	N4-Cu1-N1	159.26(16)	N16-Cu3-N13	159.19(17)
Cu2-N18	1.965(4)	N2-Cu1-N17	142.86(18)	N15-Cu3-O5	146.56(19)
Cu2-O21	2.176(4)	N2-Cu1-O11	112.17(16)	N15-Cu3-O31	114.36(16)

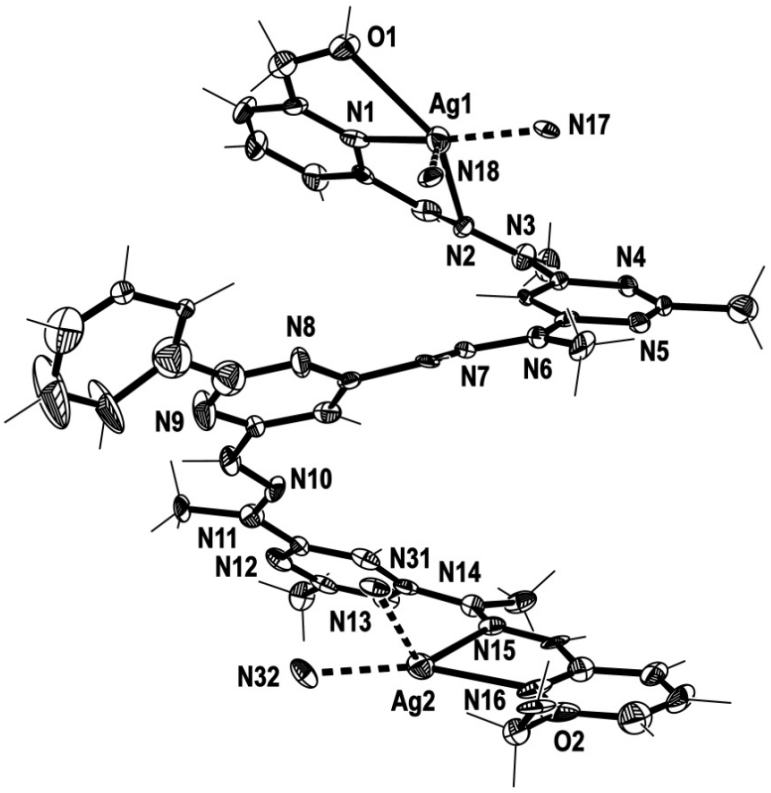

Figure S7. View of one of the **L1** molecules of the double helicate $[Ag_2\mathbf{L1}_2]^{2+}$ cation of complex **5** (crystallographic numbering). Thermal ellipsoids drawn at the 50 % probability level.

Table S7. Selected bond lengths (Å) and angles (°) of $[Ag_2\mathbf{L1}_2](SO_3CF_3)_2 \cdot CH_3CN \cdot H_2O$ (**4**).

Ag1-N1	2.267(9)	Ag2-N31	2.499(8)	N1-Ag1-N17	160.3(4)
Ag1-N2	2.637(8)	Ag2-N32	2.208(9)	N2-Ag1-O1	138.4(3)
Ag1-N17	2.246(9)	O1-Ag1-N1	69.5(3)	N15-Ag2-N16	72.3(4)
Ag1-N18	2.489(9)	N1-Ag1-N2	69.0(3)	N16-Ag2-N31	104.7(3)
Ag1-O1	2.564(7)	N2-Ag1-N17	100.9(3)	N31-Ag2-N32	71.3(4)
Ag2-N15	2.479(9)	N17-Ag1-N18	71.2(3)	N32-Ag2-N15	127.4(3)
Ag2-N16	2.240(9)	N18-Ag1-O1	85.6(3)	N16-Ag2-N32	159.0(3)

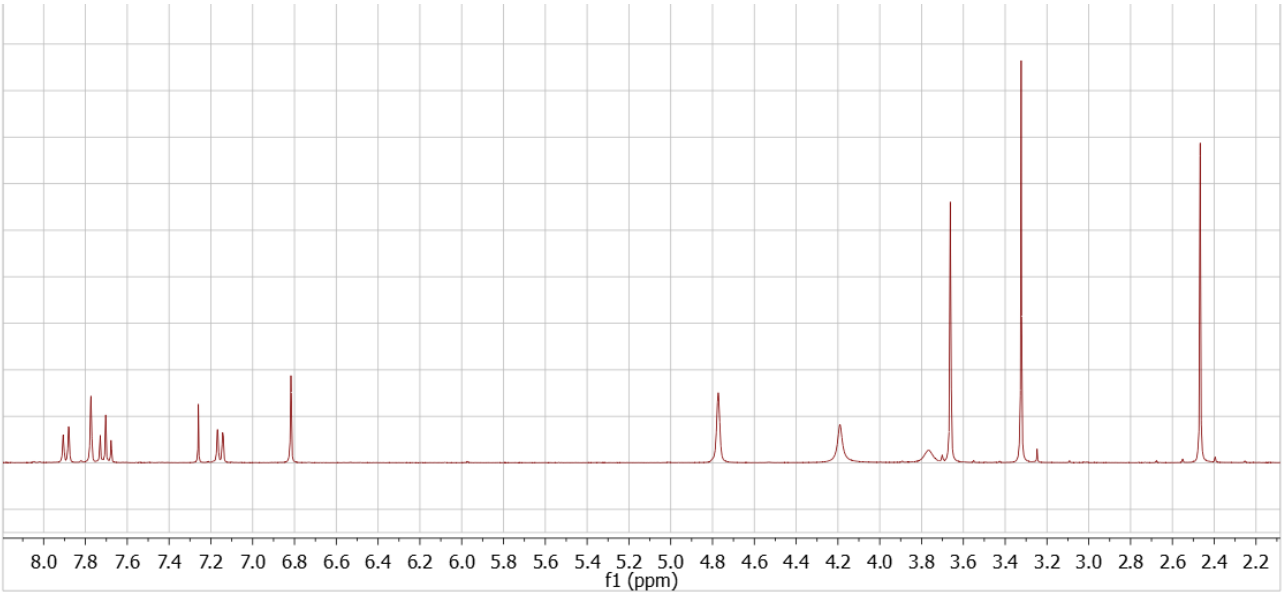

Figure S8. ^{1}H NMR spectrum of **AB** taken in $CDCl_3$ (referenced to the internal solvent signal at 7.26 ppm).

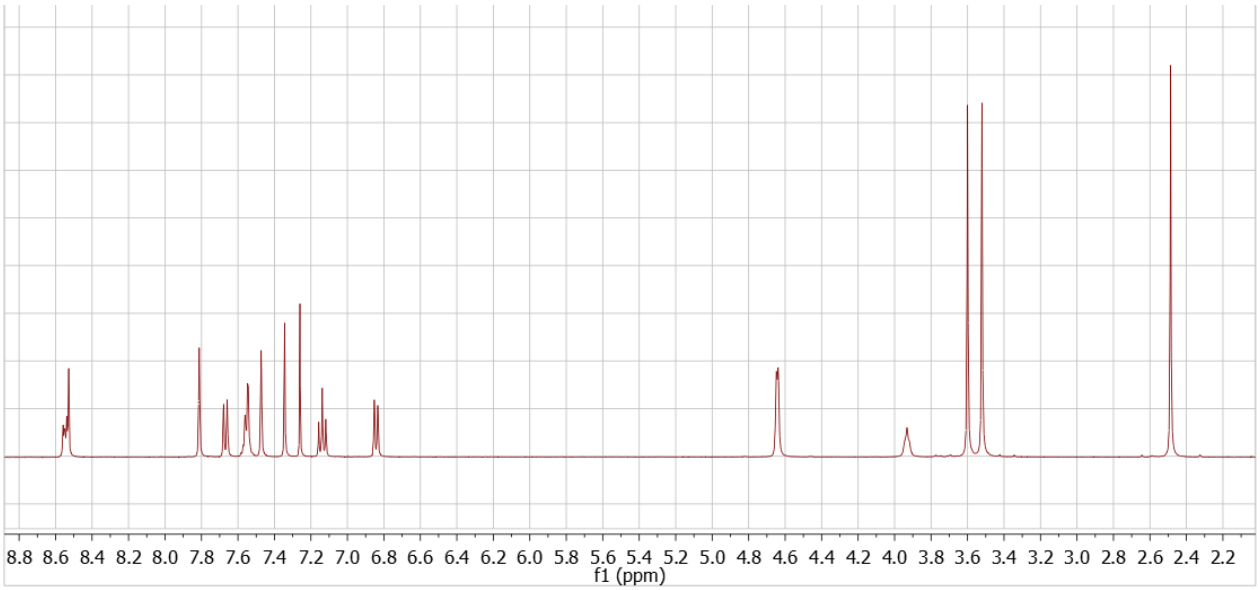

Figure S9. ^{1}H NMR spectrum of **L1** taken in $CDCl_3$ (referenced to the internal solvent signal at 7.26 ppm).

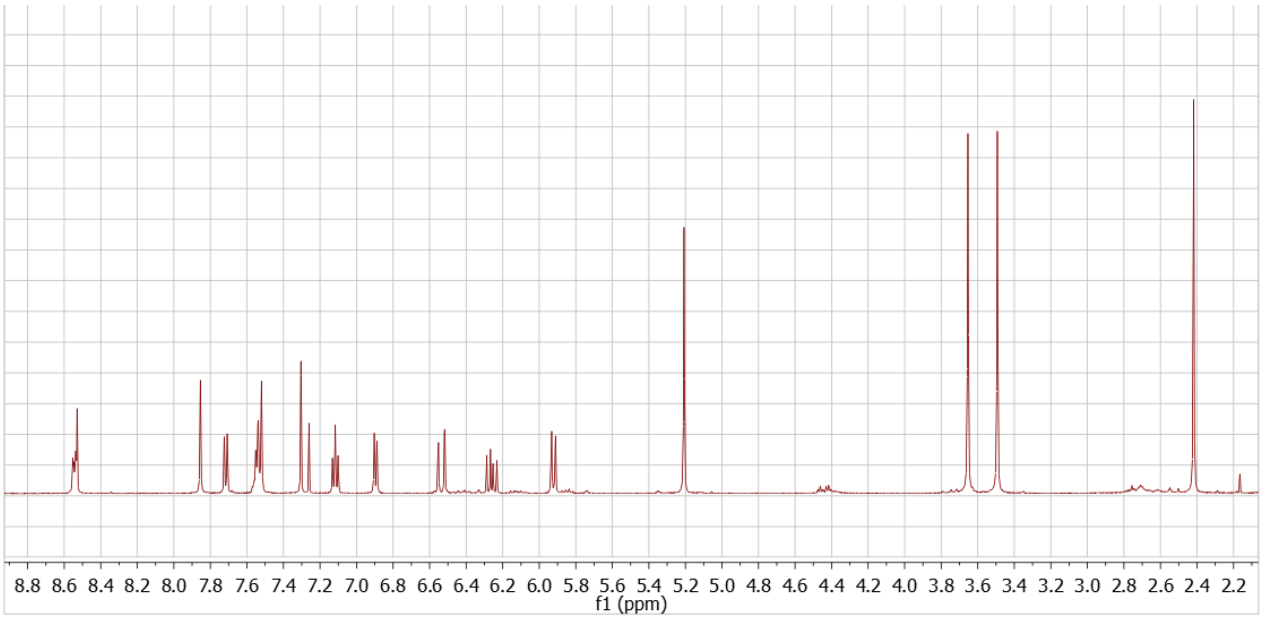

Figure S10. ^{1}H NMR spectrum of **L2** taken in $CDCl_3$ (referenced to the internal solvent signal at 7.26 ppm).

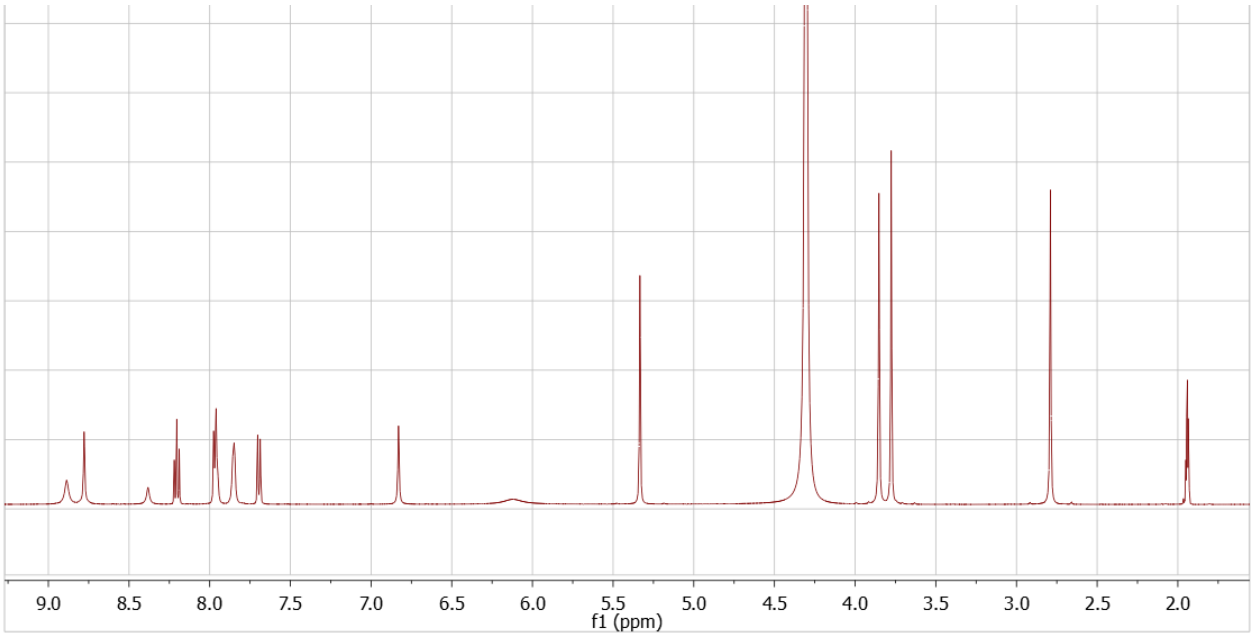

Figure S11. ^{1}H NMR spectrum of Pb_4**L1**$(ClO_4)_8$ taken in CD_3CN (referenced to the internal solvent signal at 1.94 ppm).

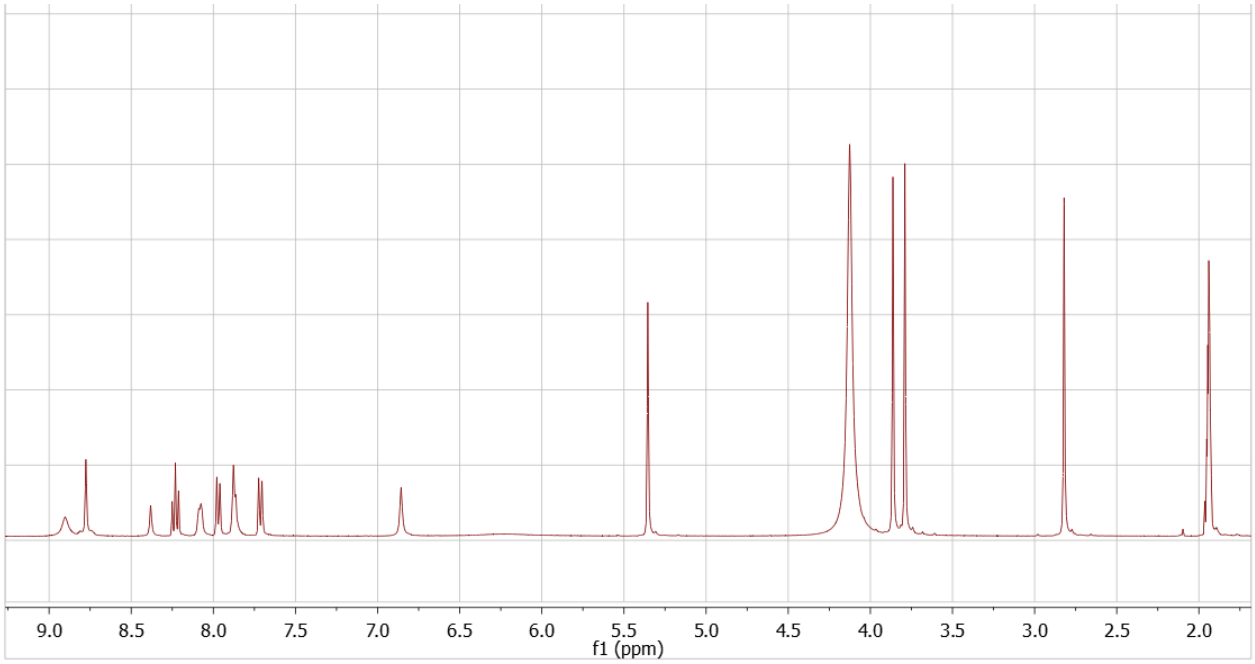

Figure S12. ^{1}H NMR spectrum of Pb_4**L1**$(SO_3CF_3)_8$ taken in CD_3CN (referenced to the internal solvent signal at 1.94 ppm).

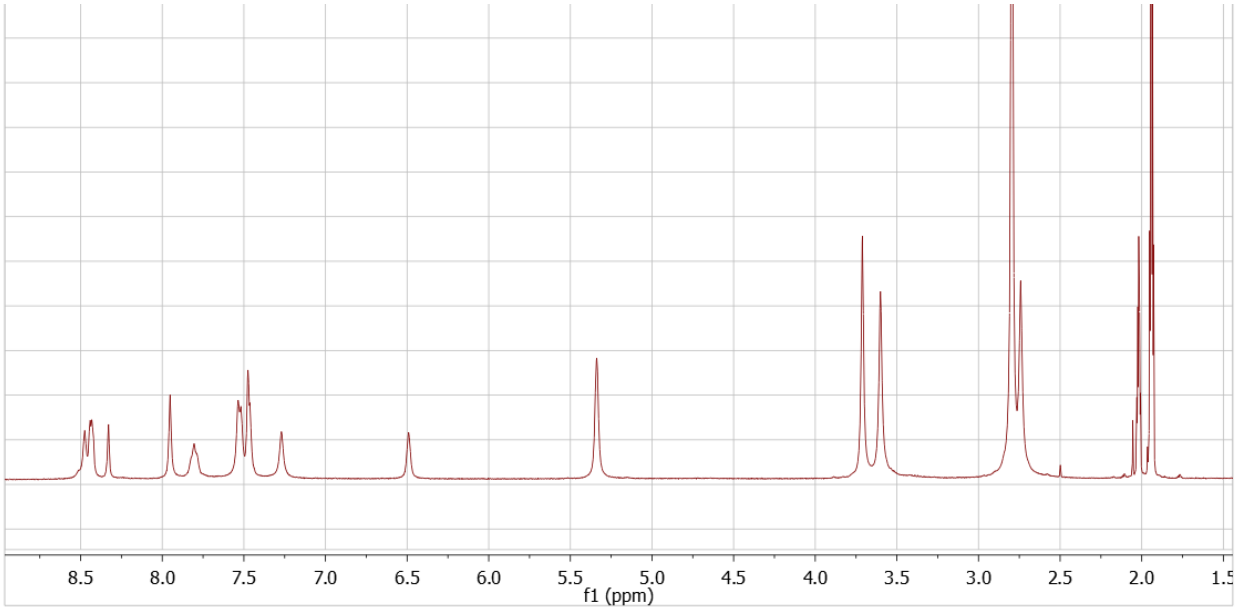

Figure S13. ^{1}H NMR spectrum of Pb_2**L1**$(ClO_4)_4$ taken in $CD_3CN/(CD_3)_2CO$ (referenced to the internal CD_3CN solvent signal at 1.94 ppm).

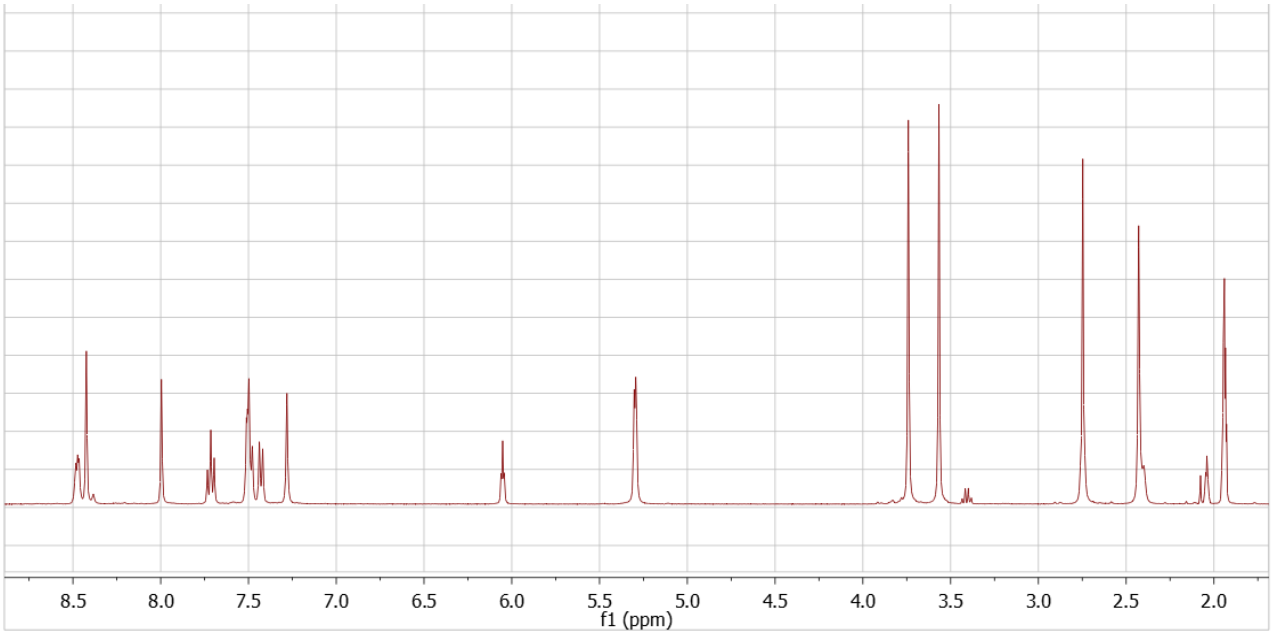

Figure S14. ^{1}H NMR spectrum of Pb_2**L1**$(SO_3CF_3)_4$ taken in $CD_3CN/(CD_3)_2CO$ (referenced to the internal CD_3CN solvent signal at 1.94 ppm).

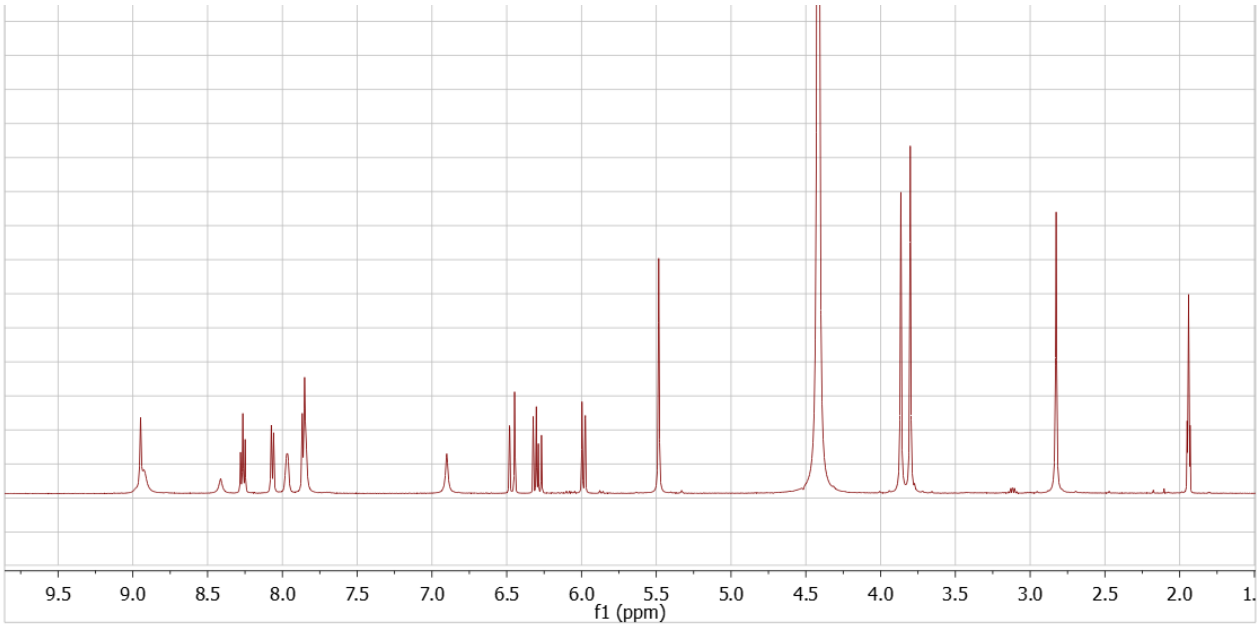

Figure S15. ^{1}H NMR spectrum of Pb_4**L2**$(ClO_4)_8$ taken in CD_3CN (referenced to the internal solvent signal at 1.94 ppm).

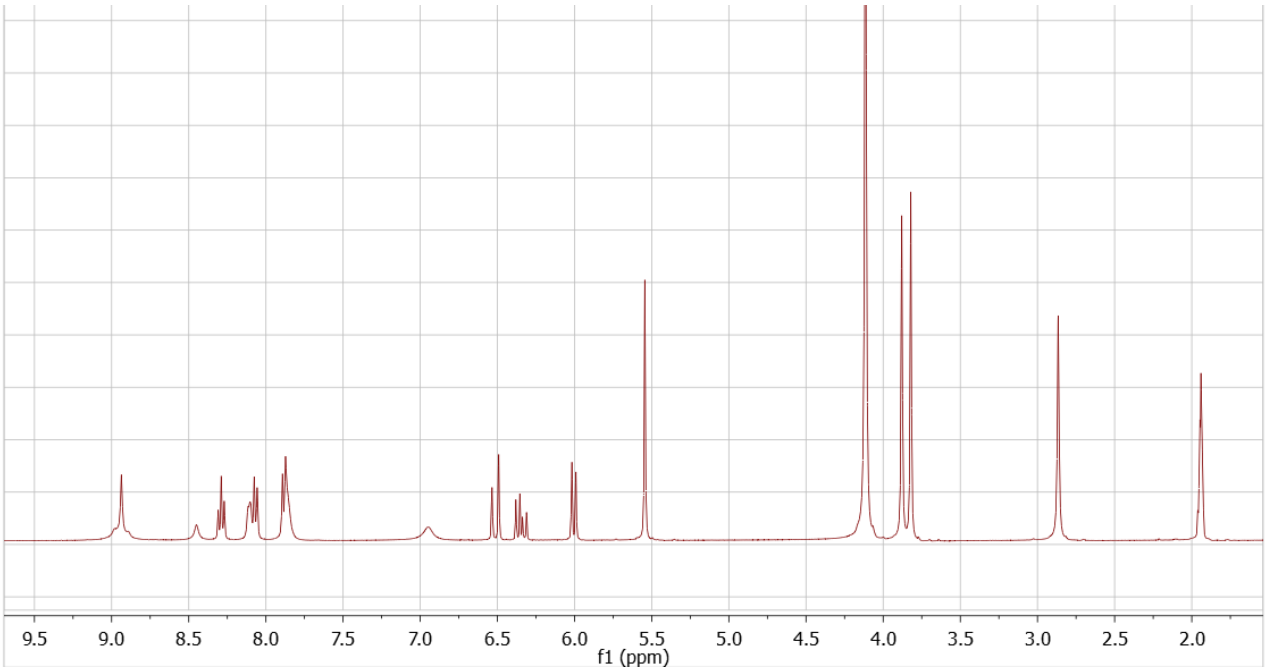

Figure S16. ^{1}H NMR spectrum of Pb_4**L2**$(SO_3CF_3)_8$ taken in CD_3CN (referenced to the internal solvent signal at 1.94 ppm).

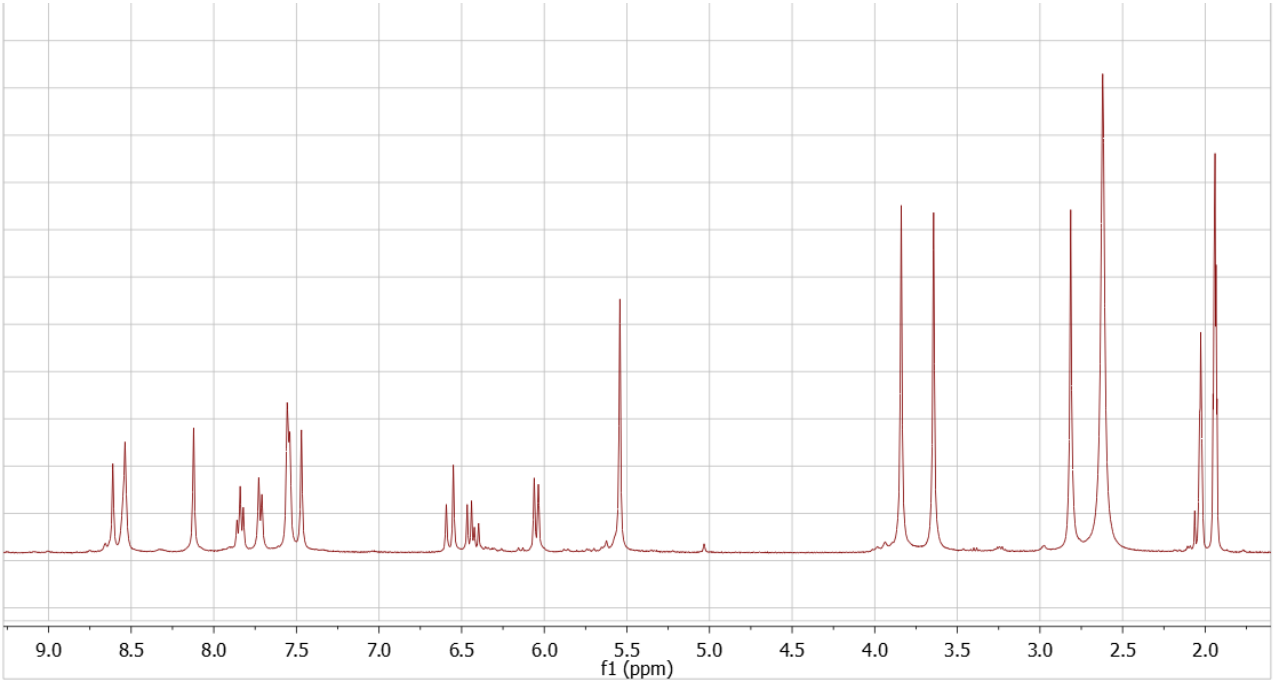

Figure S17. ^{1}H NMR spectrum of Pb_2**L2**$(ClO_4)_4$ taken in $CD_3CN/(CD_3)_2CO$ (referenced to the internal CD_3CN solvent signal at 1.94 ppm).

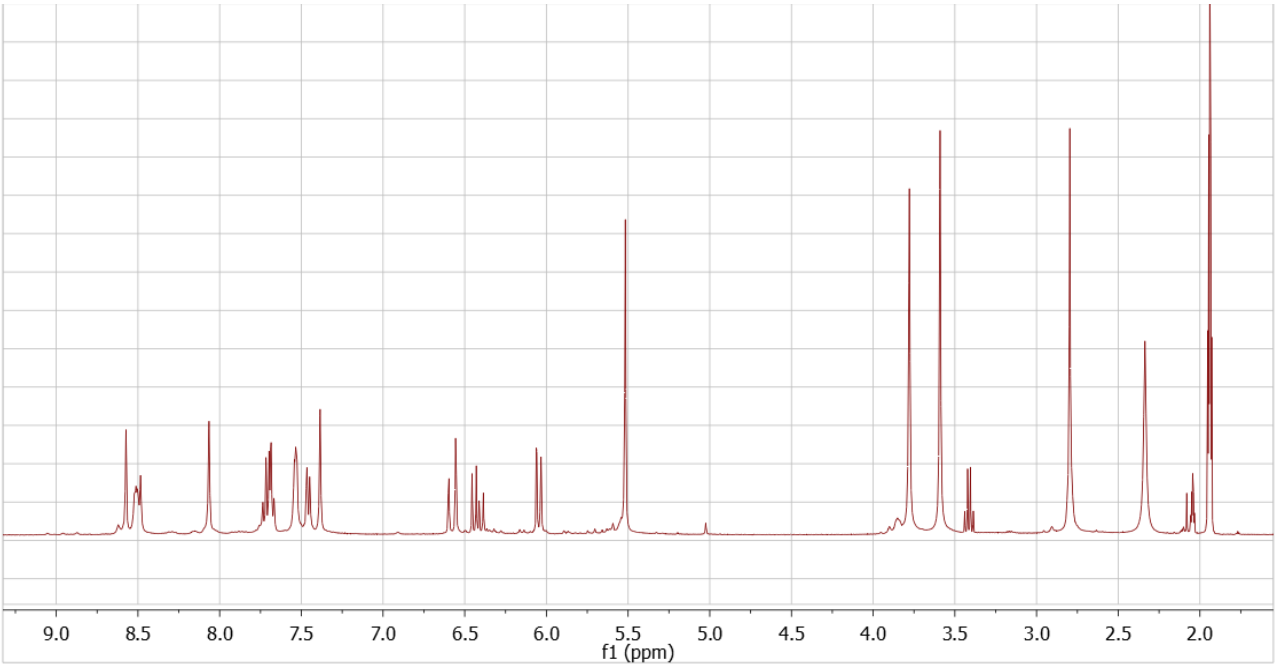

Figure S18. ^{1}H NMR spectrum of Pb_2**L2**$(SO_3CF_3)_4$ taken in $CD_3CN/(CD_3)_2CO$ (referenced to the internal CD_3CN solvent signal at 1.94 ppm).

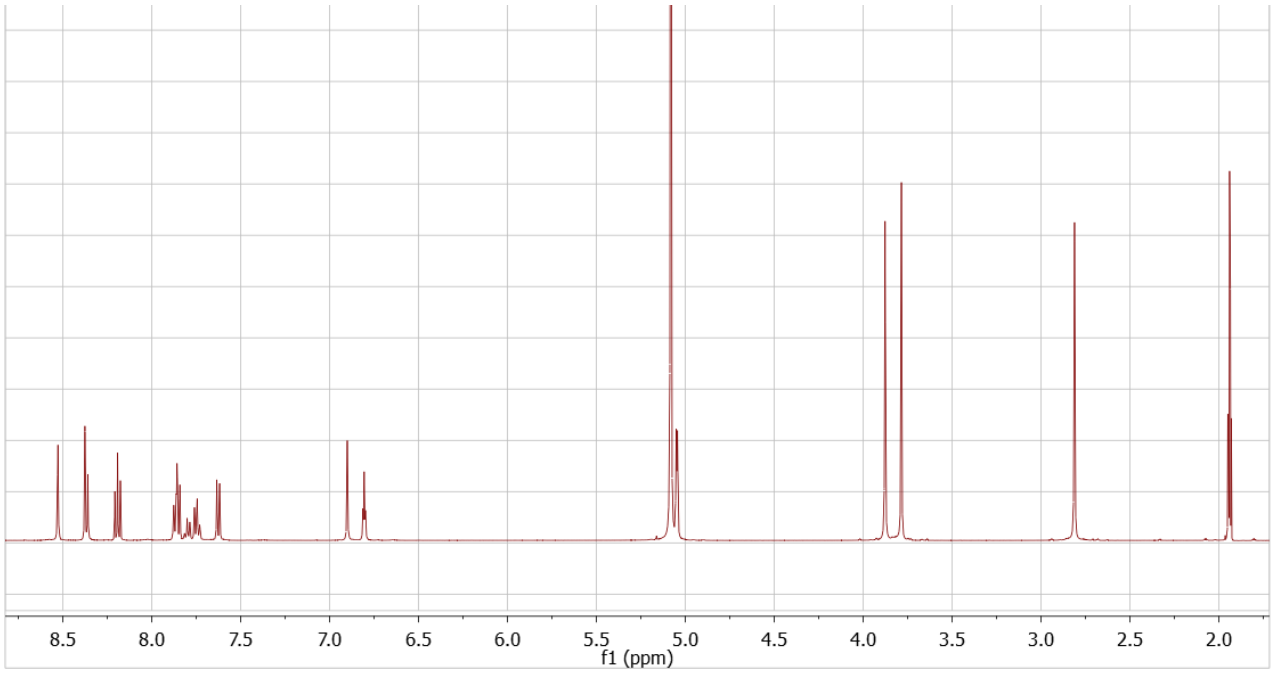

Figure S19. ^{1}H NMR spectrum of Zn_4**L1**$(SO_3CF_3)_8$ taken in CD_3CN (referenced to the internal solvent signal at 1.94 ppm).

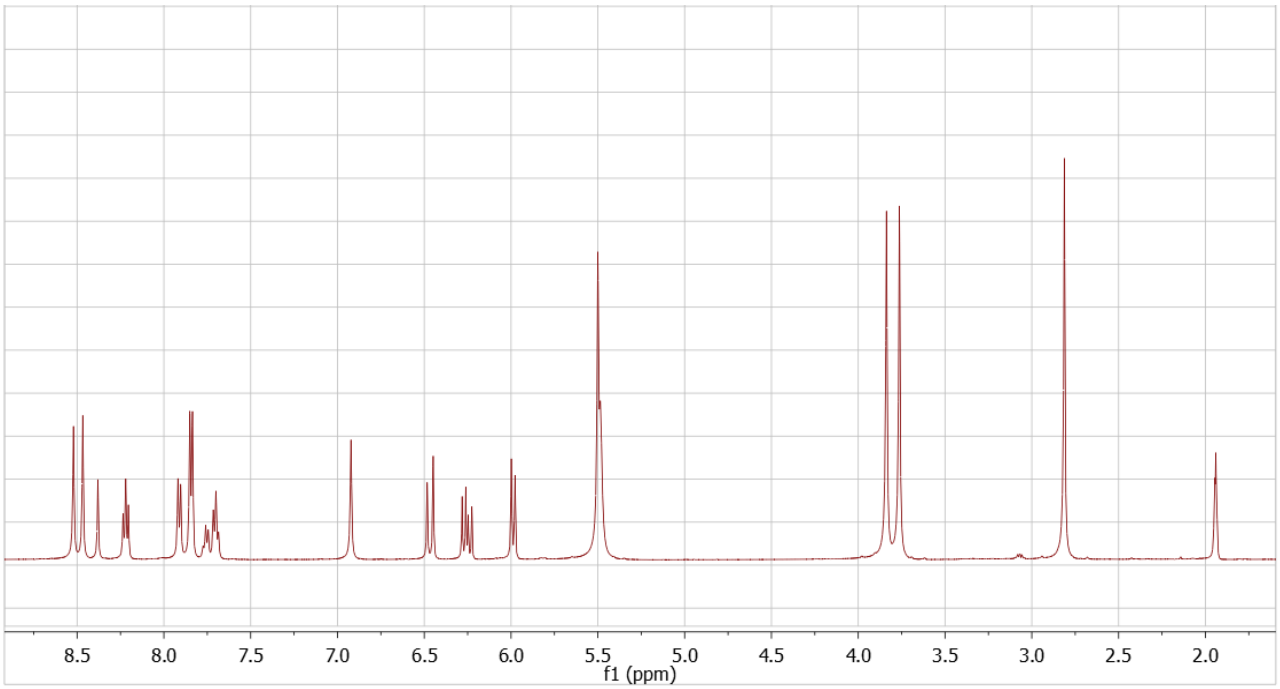

Figure S20. ^{1}H NMR spectrum of Zn_4**L2**$(SO_3CF_3)_8$ taken in CD_3CN (referenced to the internal solvent signal at 1.94 ppm).

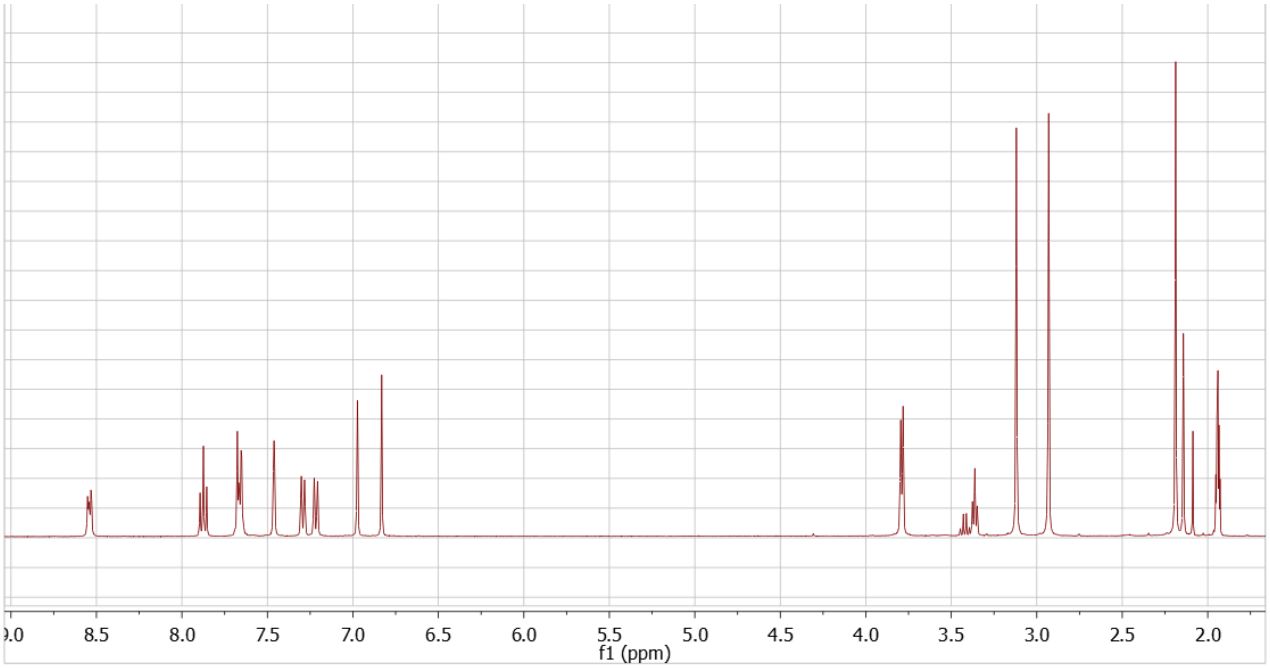

Figure S21. ^{1}H NMR spectrum of Ag_2**L1**$_2(SO_3CF_3)_2$ taken in CD_3CN (referenced to the internal solvent signal at 1.94 ppm).

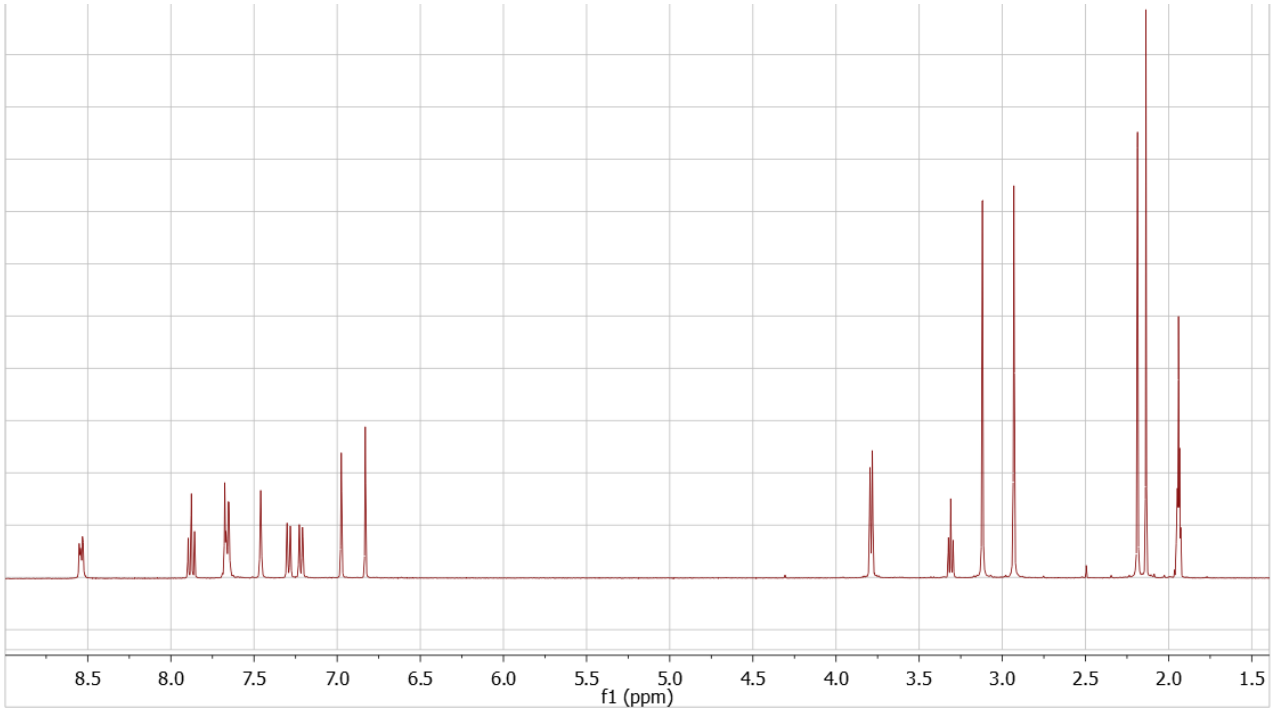

Figure S22. ^{1}H NMR spectrum of Ag_2**L1**$_2(BF_4)_2$ taken in CD_3CN (referenced to the internal solvent signal at 1.94 ppm).

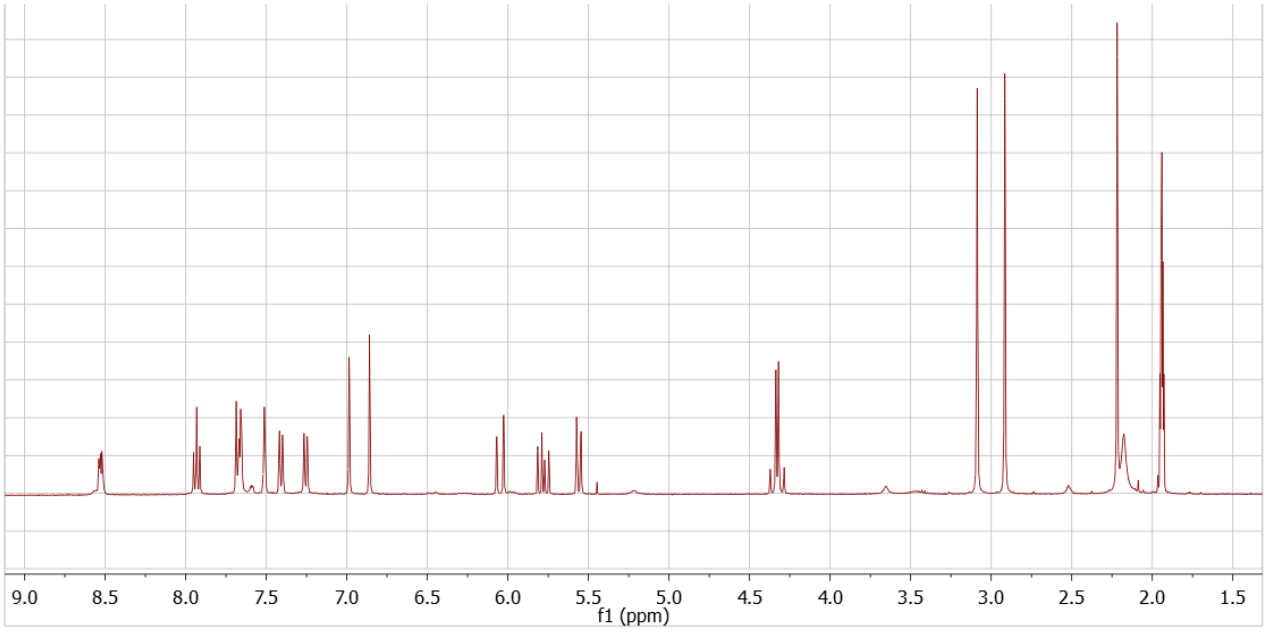

Figure S23. ^{1}H NMR spectrum of Ag_2**L2**$_2(SO_3CF_3)_2$ taken in CD_3CN (referenced to the internal solvent signal at 1.94 ppm).

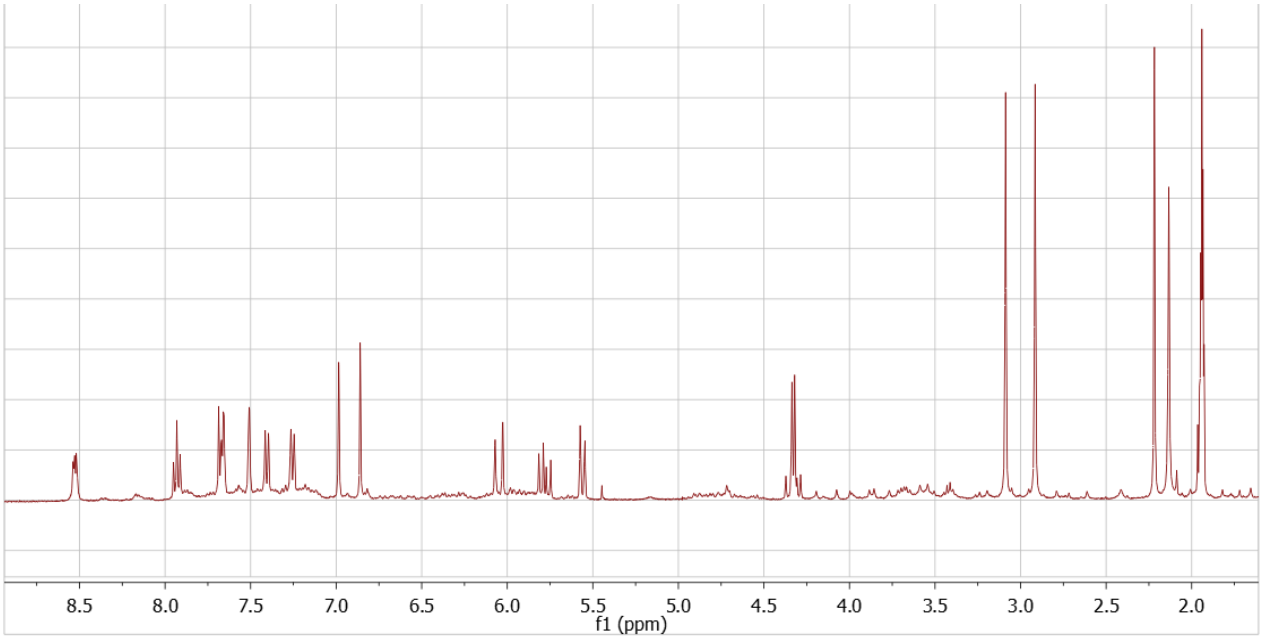

Figure S24. ^{1}H NMR spectrum of Ag_2**L2**$_2(BF_4)_2$ taken in CD_3CN (referenced to the internal solvent signal at 1.94 ppm).

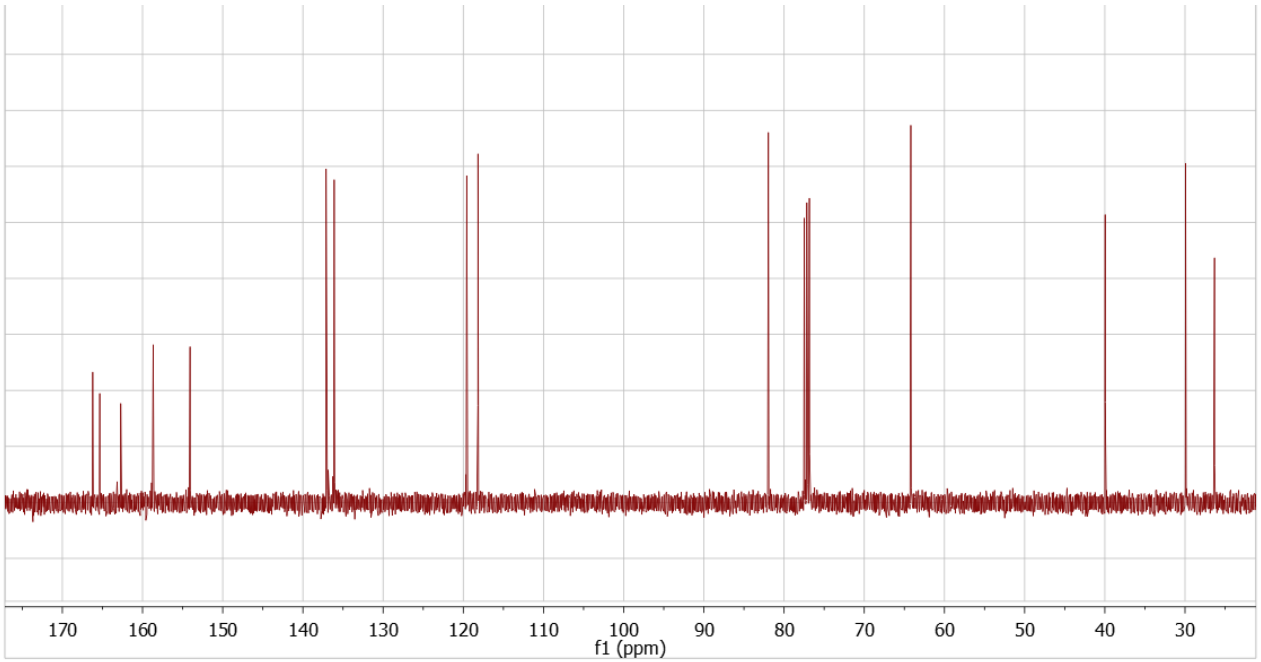

Figure S25. ^{13}C NMR spectrum of **AB** taken in $CDCl_3$ (referenced to the internal solvent signal at 77.16 ppm).

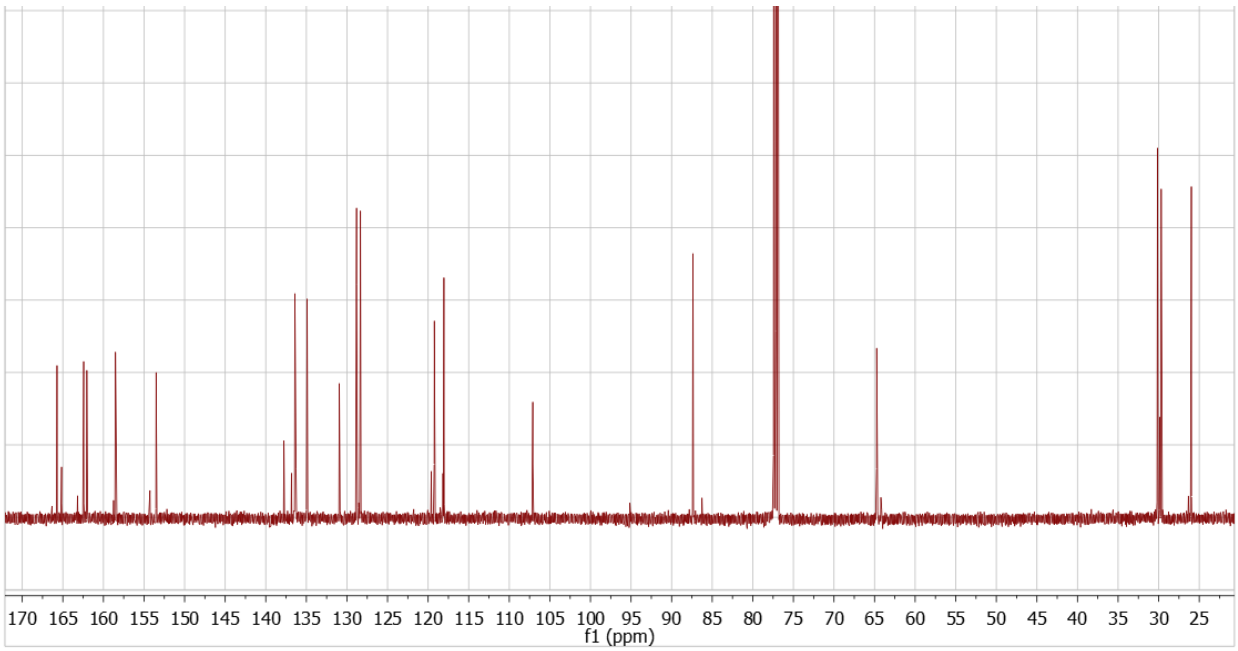

Figure S26. ^{13}C NMR spectrum of **L1** taken in $CDCl_3$ (referenced to the internal solvent signal at 77.16 ppm).

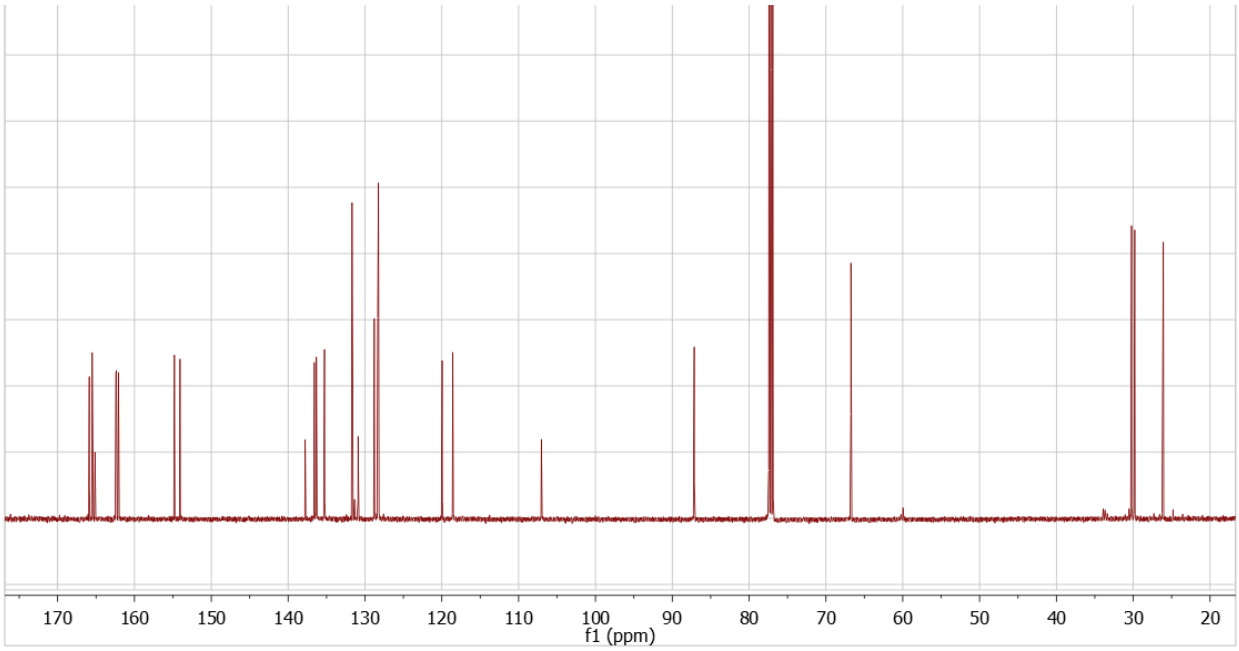

Figure S27. ^{13}C NMR spectrum of **L2** taken in $CDCl_3$ (referenced to the internal solvent signal at 77.16 ppm).

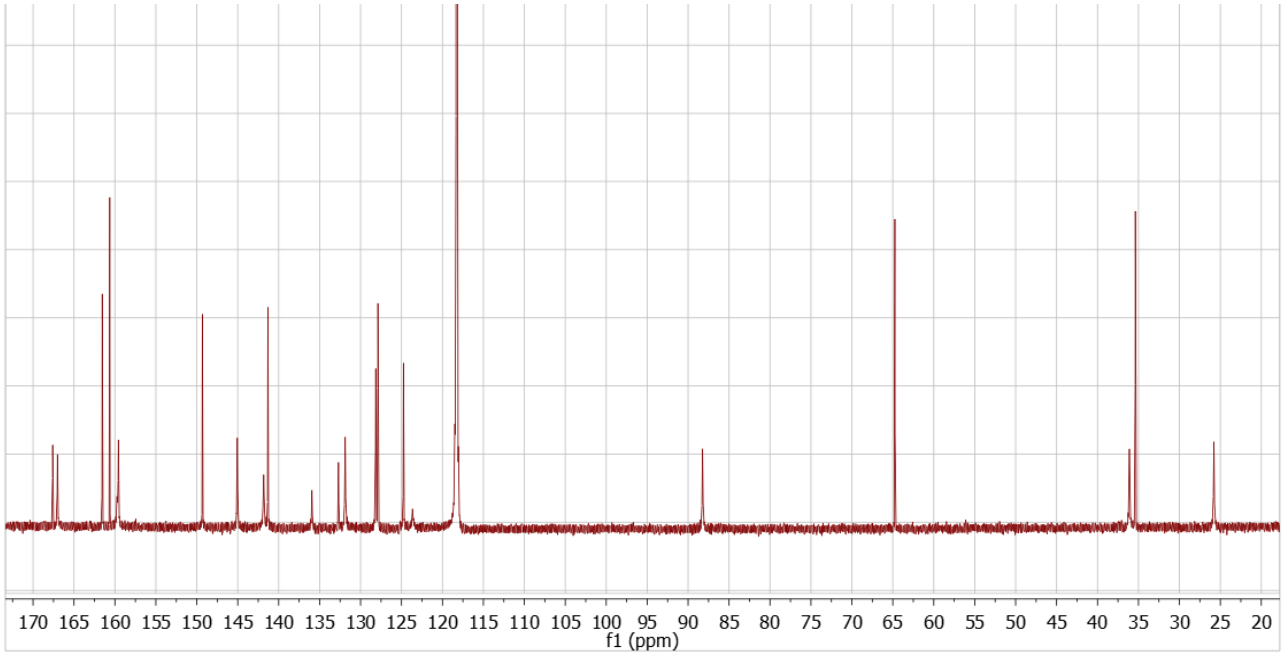

Figure S28. ^{13}C NMR spectrum of Pb_4**L1**$(ClO_4)_8$ taken in CD_3CN (referenced to the internal solvent signal at 118.26 ppm).

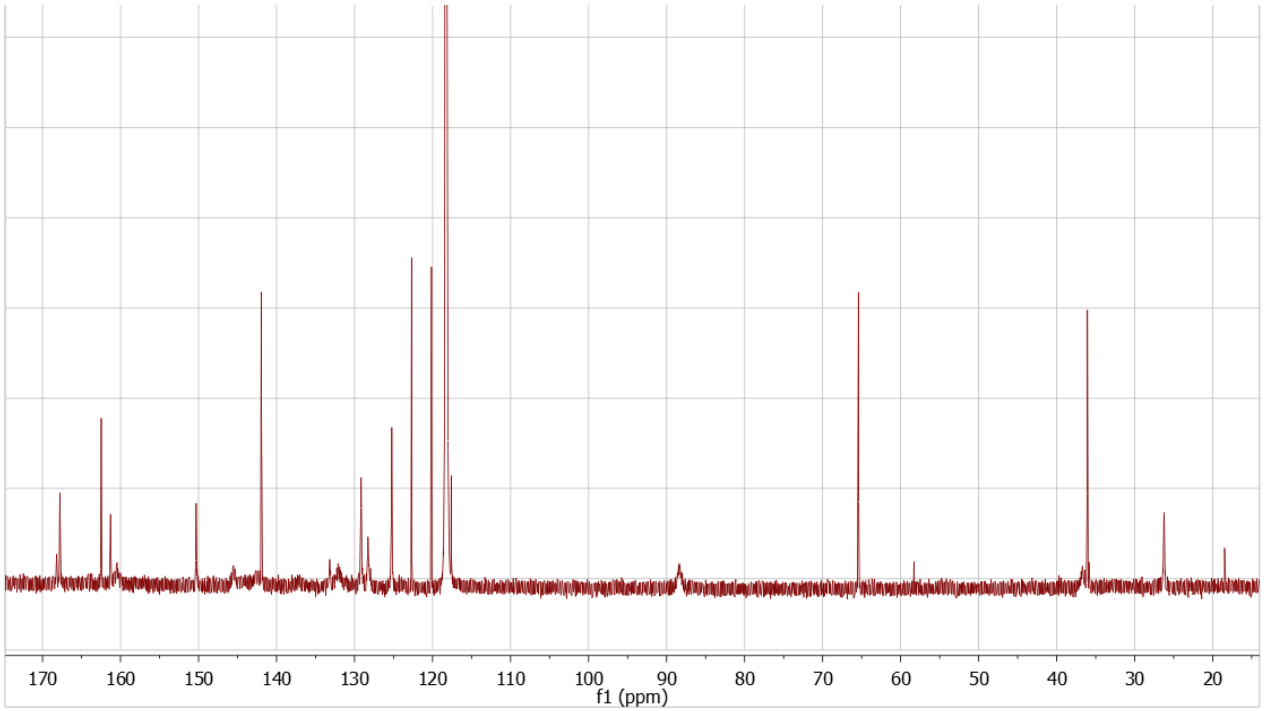

Figure S29. ^{13}C NMR spectrum of Pb_4**L1**$(SO_3CF_3)_8$ taken in CD_3CN (referenced to the internal solvent signal at 118.26 ppm).

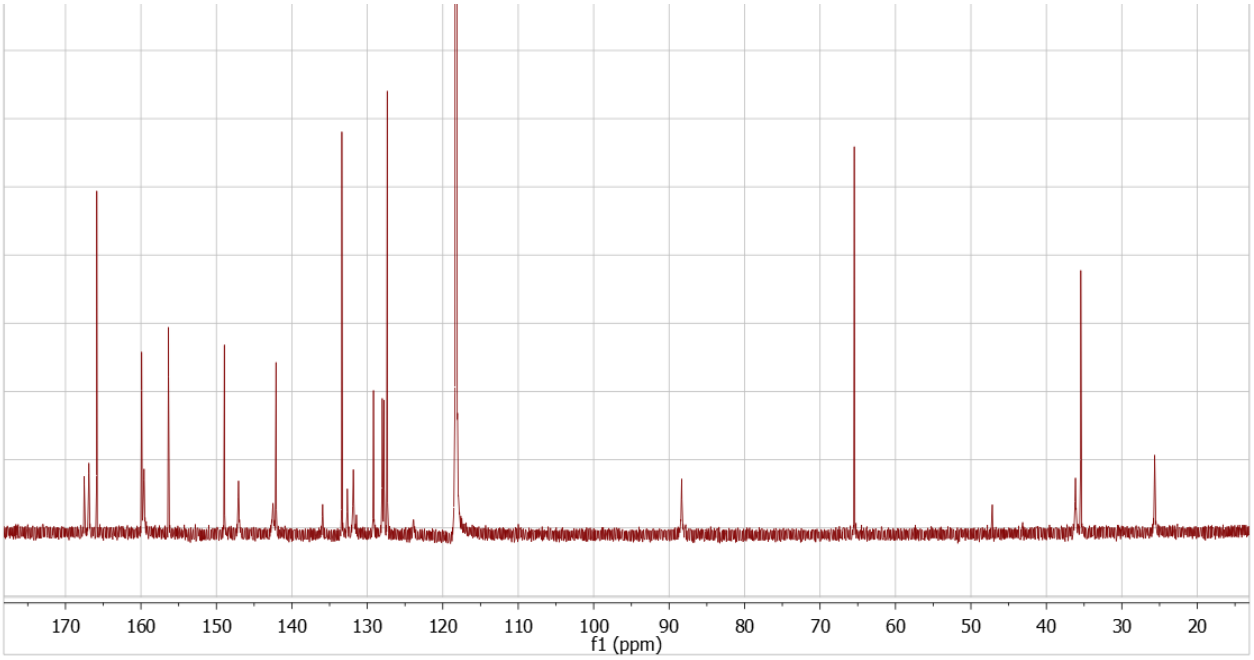

Figure S30. ^{13}C NMR spectrum of Pb_4**L2**$(ClO_4)_8$ taken in CD_3CN (referenced to the internal solvent signal at 118.26 ppm).

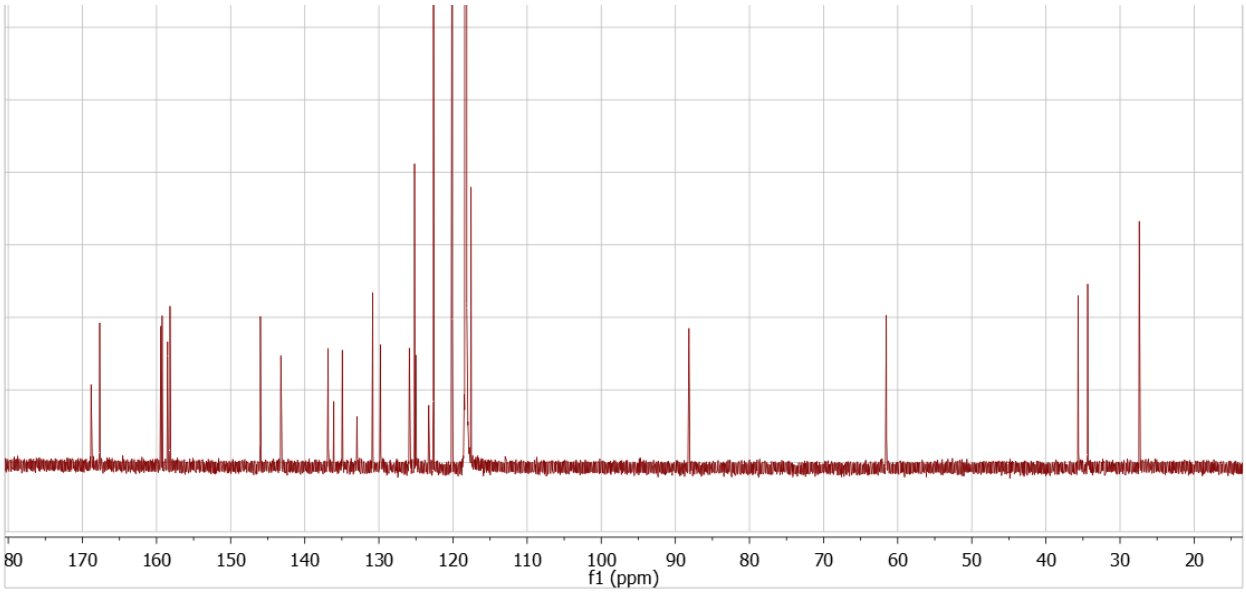

Figure S31. ^{13}C NMR spectrum of Zn_4**L1**$(SO_3CF_3)_8$ taken in CD_3CN (referenced to the internal solvent signal at 118.26 ppm).

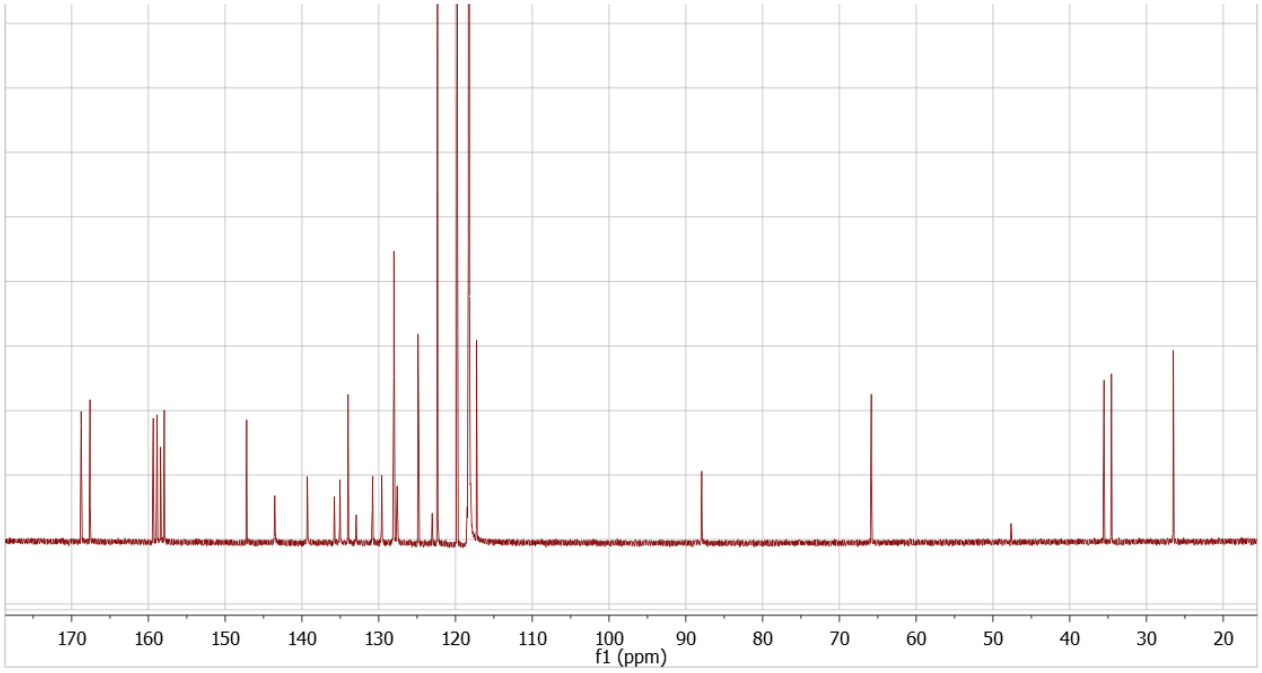

Figure S32. ^{13}C NMR spectrum of Zn_4**L2**$(SO_3CF_3)_8$ taken in CD_3CN (referenced to the internal solvent signal at 118.26 ppm).

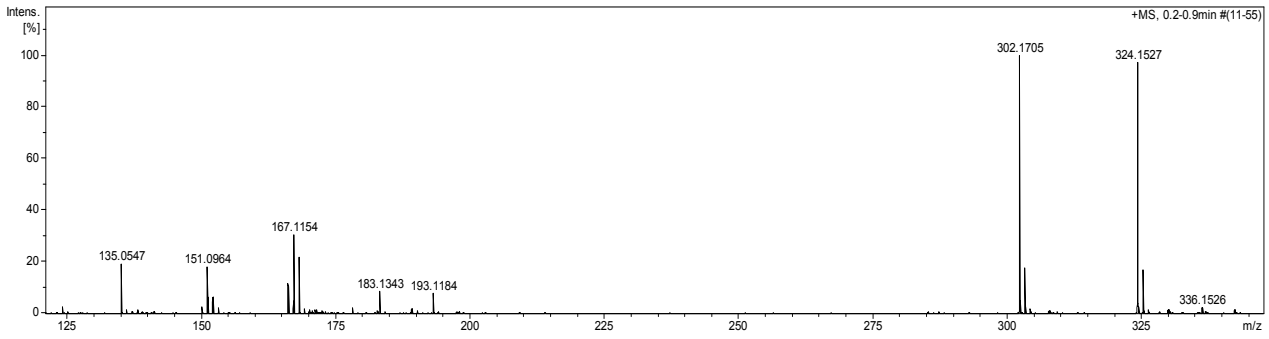

Figure S33. ESMS spectrum of **AB**.

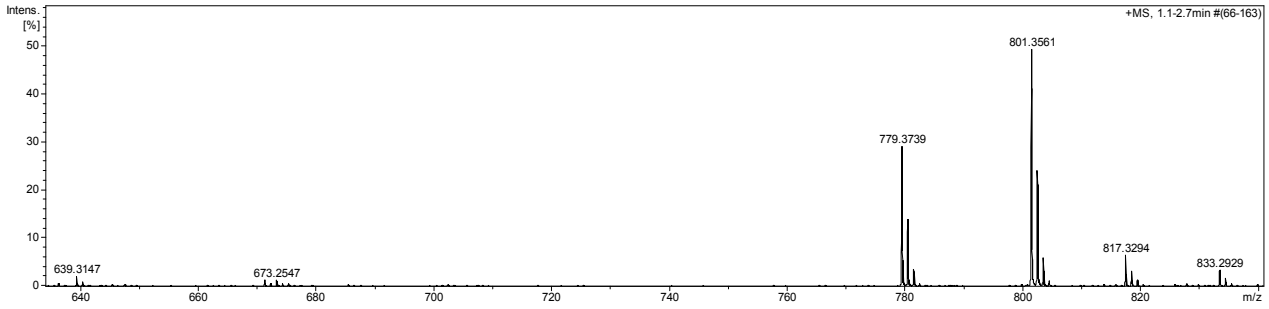

Figure S34. ESMS spectrum of **L1**.

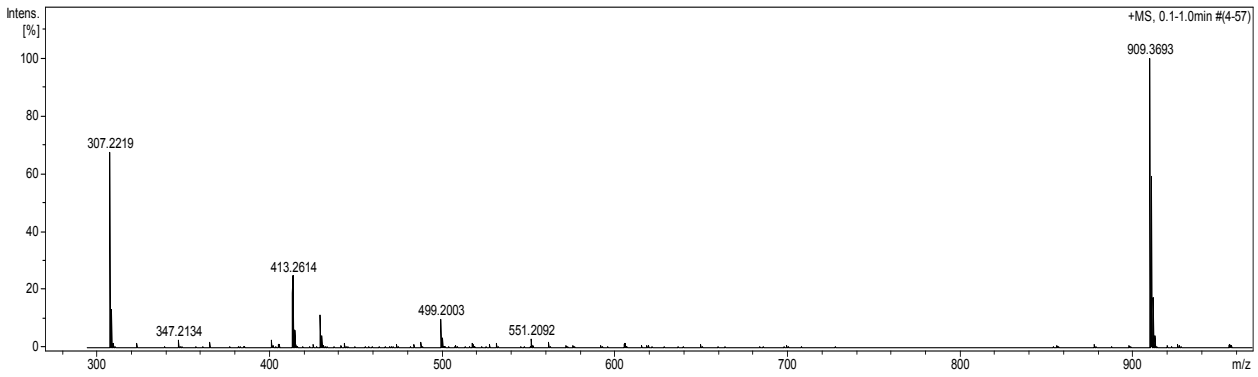

Figure S35. ESMS spectrum of **L2**.

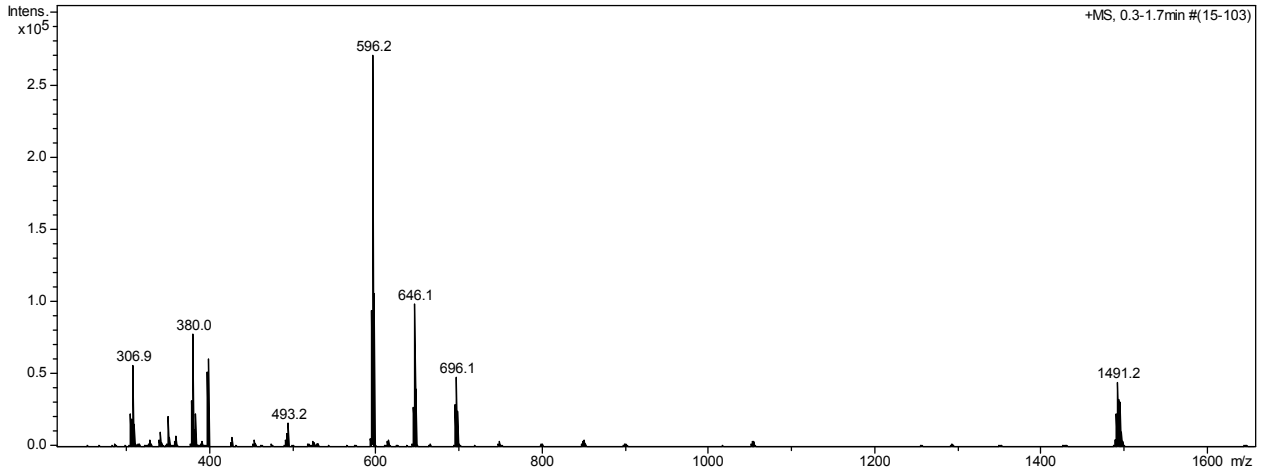

Figure S36. ESMS spectrum of Pb_4**L1**$(ClO_4)_8$.

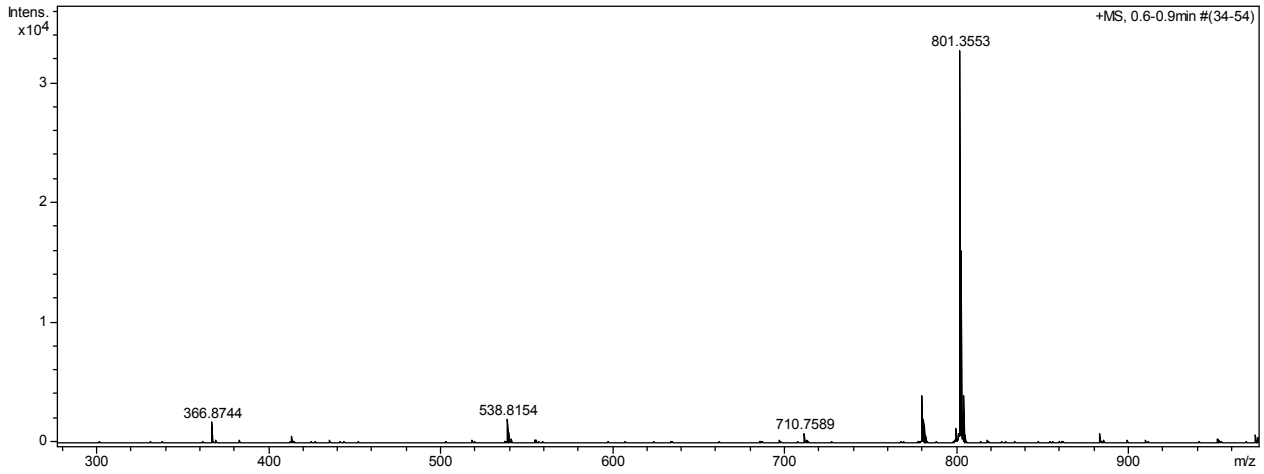

Figure S37. ESMS spectrum of Pb_4**L1**$(SO_3CF_3)_8$.

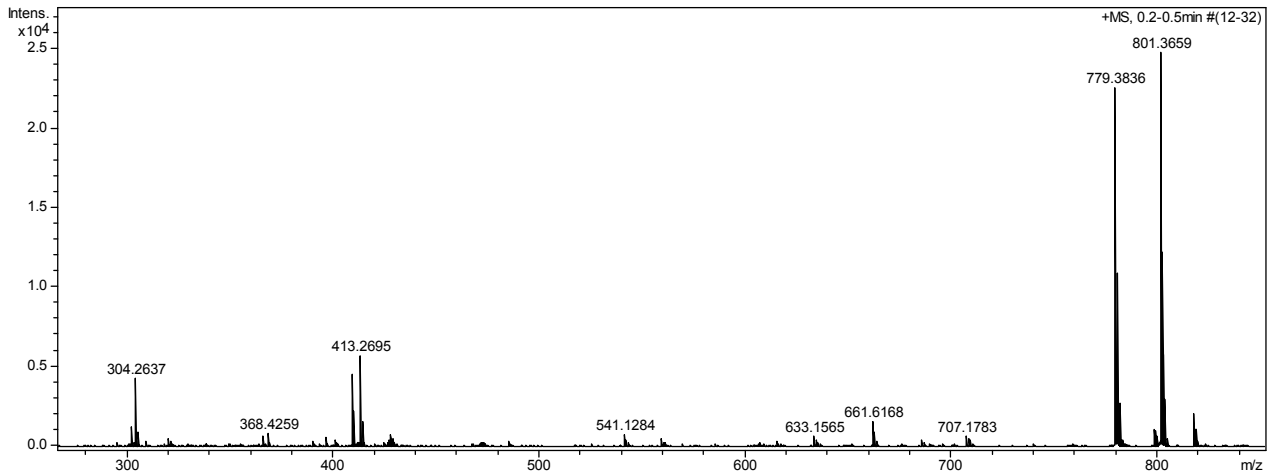

Figure S38. ESMS spectrum of Pb_2**L1**$(ClO_4)_4$.

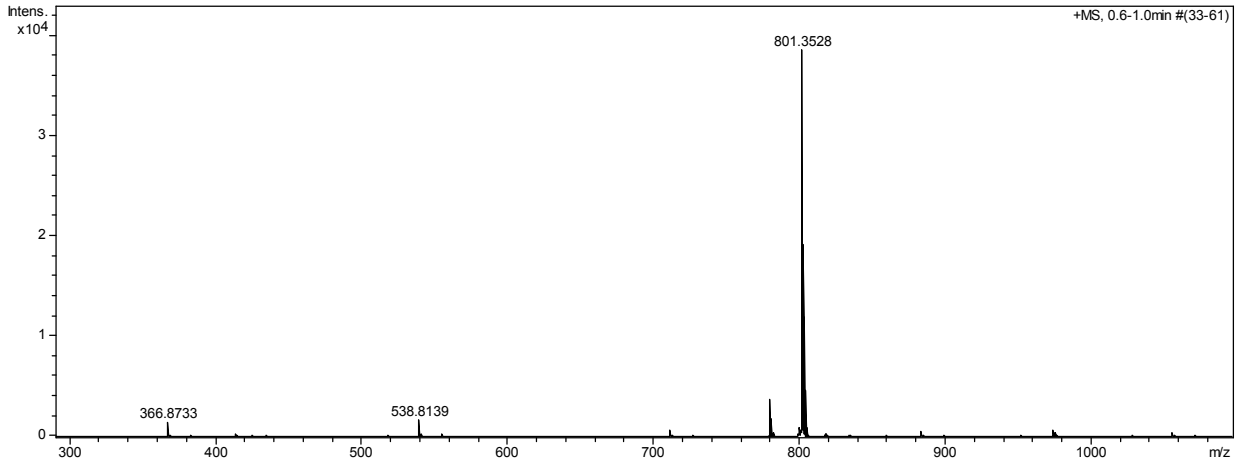

Figure S39. ESMS spectrum of Pb_2**L1**$(SO_3CF_3)_4$.

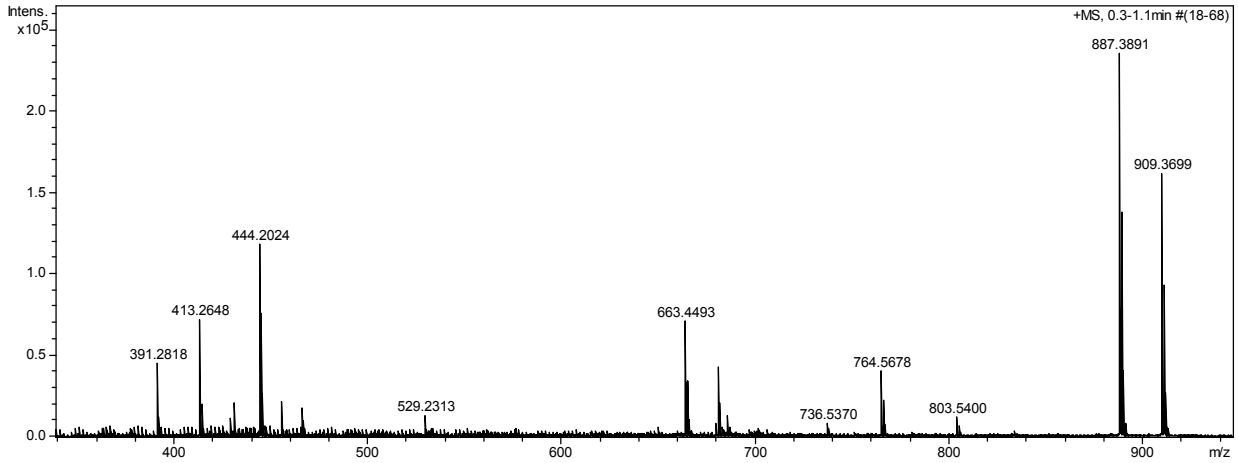

Figure S40. ESMS spectrum of Pb_4**L2**$(ClO_4)_8$.

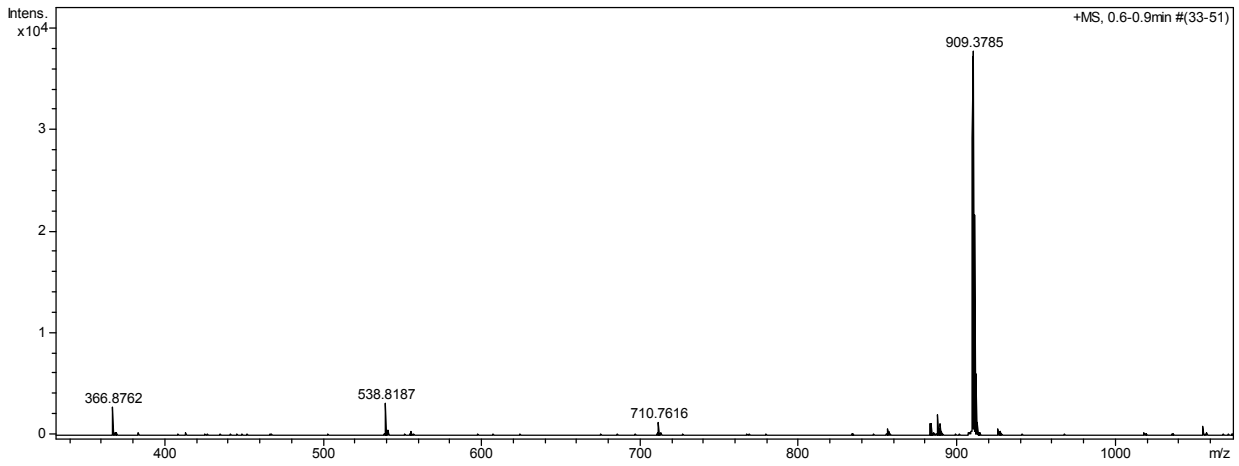

Figure S41. ESMS spectrum of Pb_4**L2**$(SO_3CF_3)_8$.

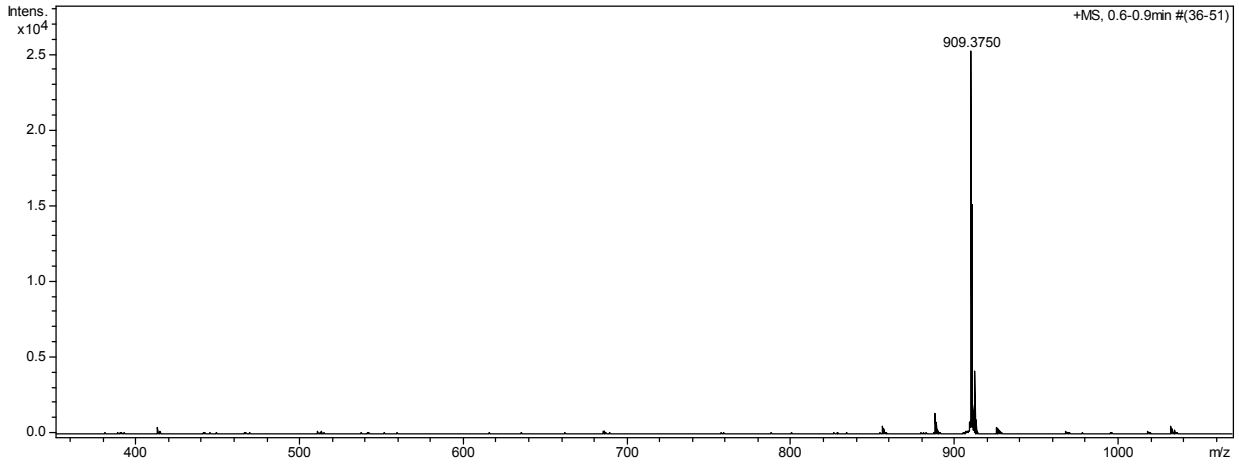

Figure S42. ESMS spectrum of Pb_2**L2**$(ClO_4)_4$.

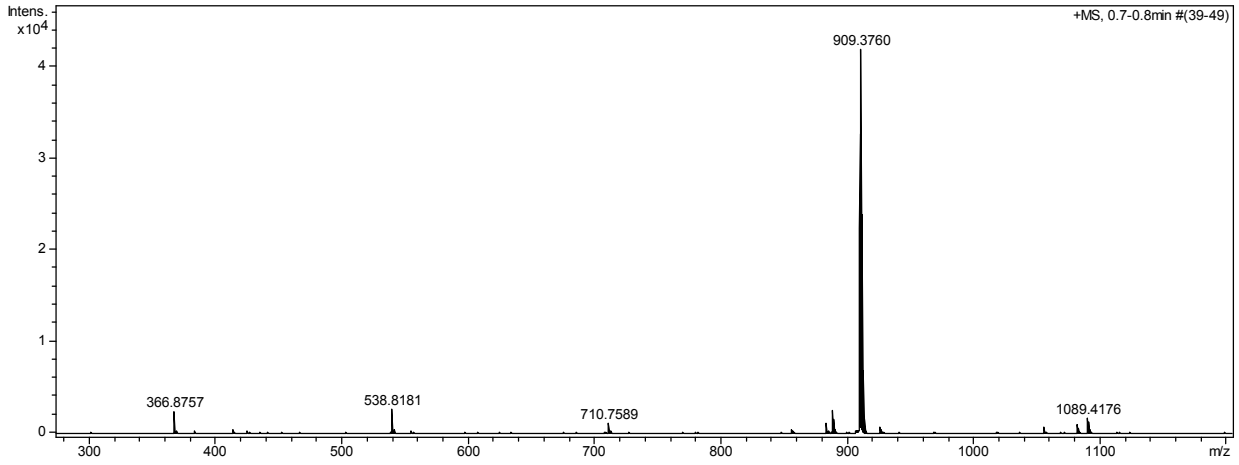

Figure S43. ESMS spectrum of Pb_2**L2**$(SO_3CF_3)_4$.

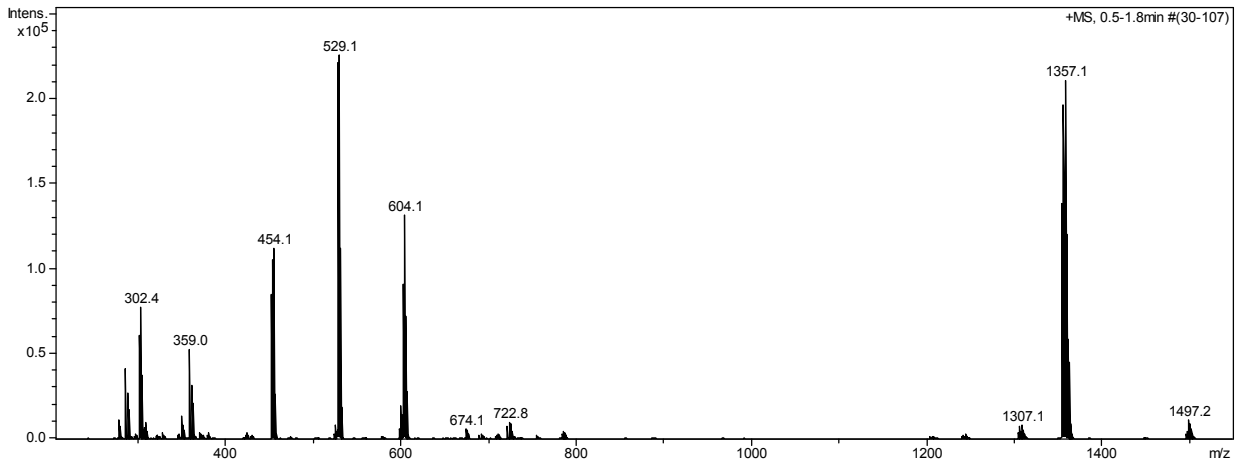

Figure S44. ESMS spectrum of Zn_4**L1**$(SO_3CF_3)_8$.

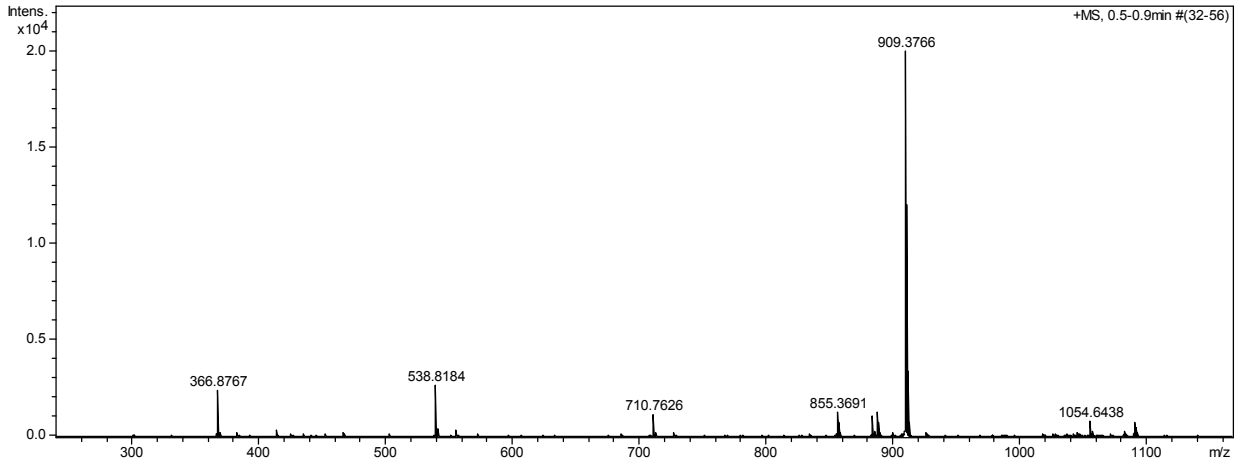

Figure S45. ESMS spectrum of Zn_4**L2**$(SO_3CF_3)_8$.

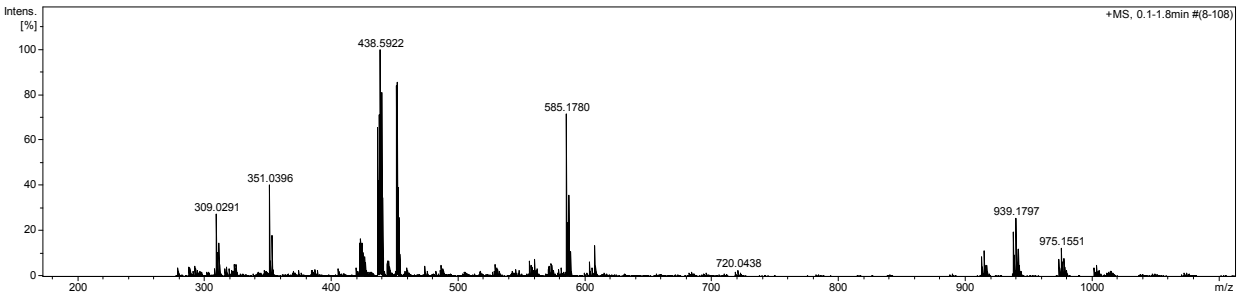

Figure S46. ESMS spectrum of Cu_4**L1**$(ClO_4)_8$

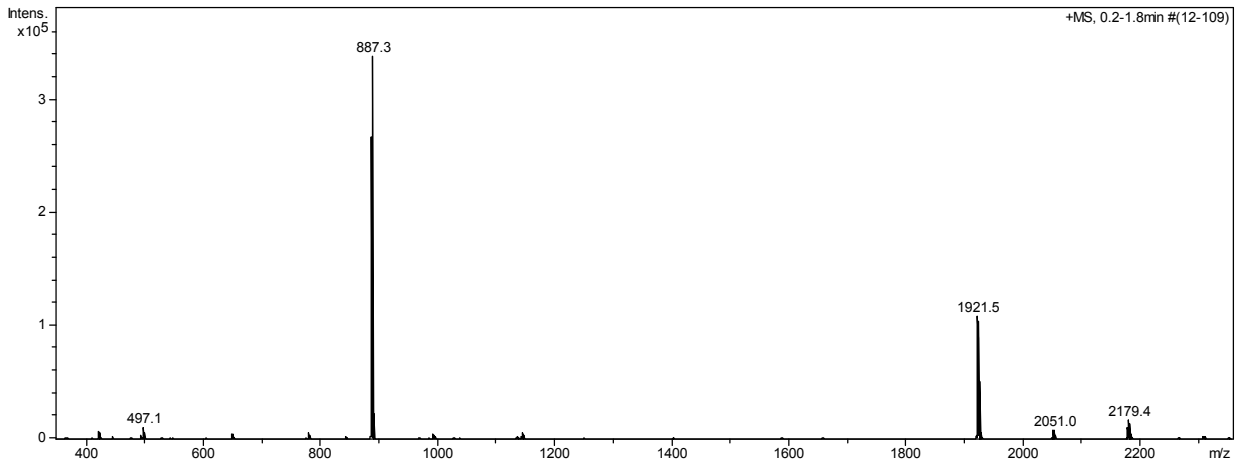

Figure S47. ESMS spectrum of $Ag_2\mathbf{L1}_2(SO_3CF_3)_2$.

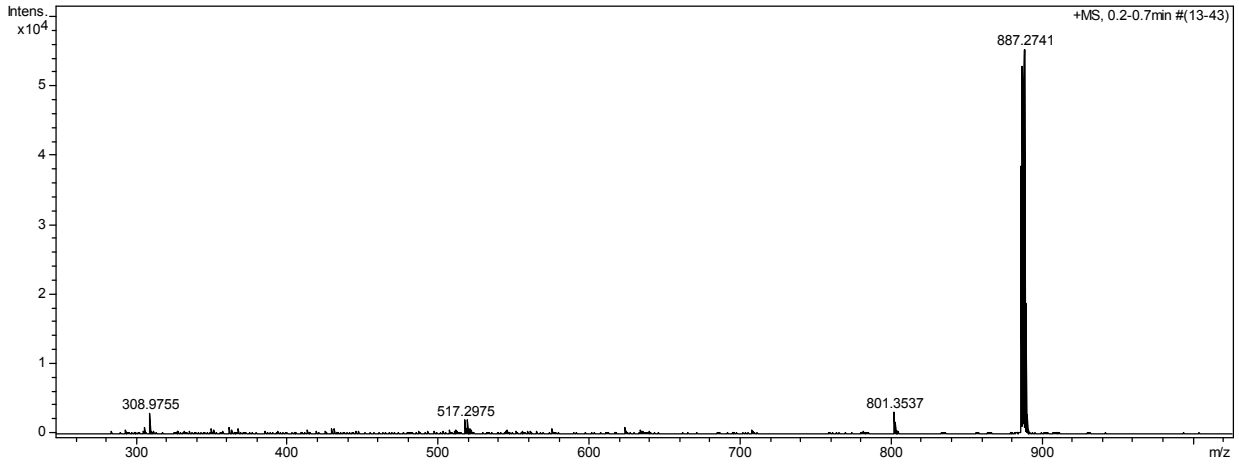

Figure S48. ESMS spectrum of $Ag_2\mathbf{L1}_2(BF_4)_2$.

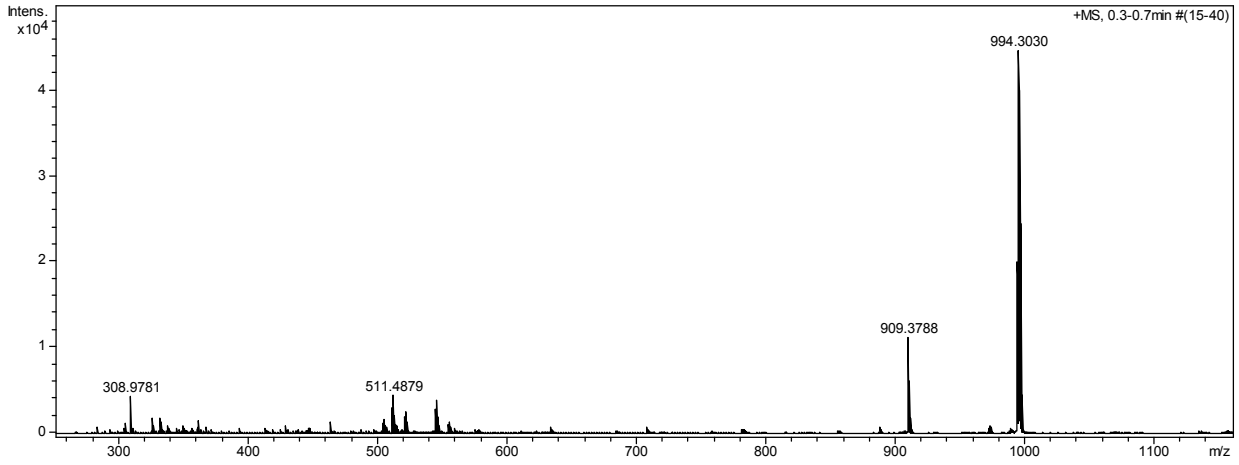

Figure S49. ESMS spectrum of $Ag_2\mathbf{L2}_2(SO_3CF_3)_2$.

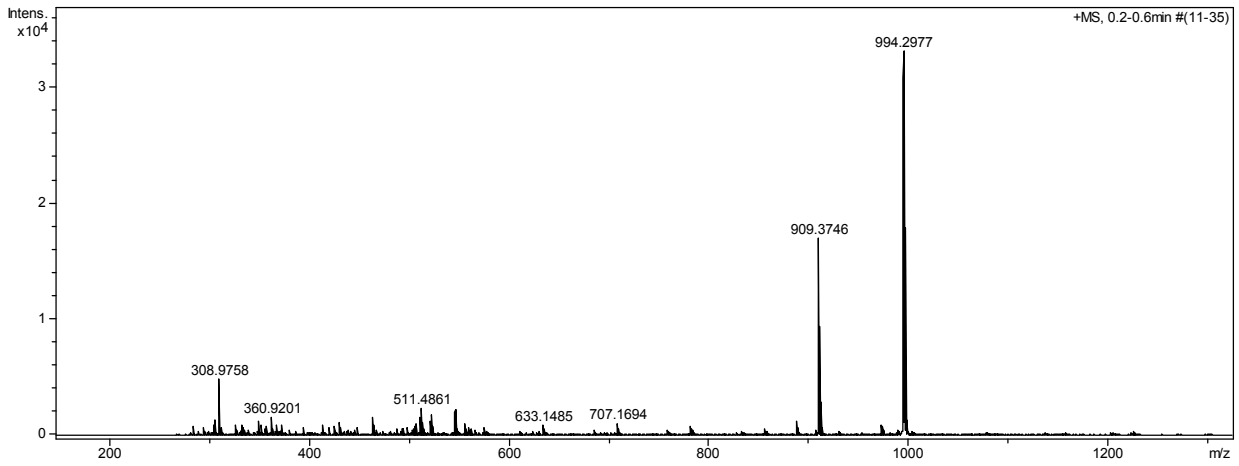

Figure S50. ESMS spectrum of $Ag_2\mathbf{L2}_2(BF_4)_2$.